2012

Keggin-type aluminum nanoclusters: synthesis, structural characterization and environmental implications

Samangi Abeysinghe
University of Iowa

KEGGIN-TYPE ALUMINUM NANOCLUSTERS: SYNTHESIS, STRUCTURAL CHARACTERIZATION AND ENVIRONMENTAL IMPLICATIONS

by

Samangi Abeysinghe

A thesis submitted in the partial fulfillment of the
requirements for the
Master of Science degree in Chemistry
in the Graduate College of
The University of Iowa

May 2012

Thesis Supervisor: Assistant Professor Tori Z. Forbes

Graduate College
The University of Iowa
Iowa City, Iowa

CERTIFICATE OF APPROVAL

MASTER'S THESIS

This is to certify that the Master's thesis of

Samangi Abeysinghe

has been approved by the Examining Committee for the thesis requirement for the Master of Science degree in Chemistry at the May 2012 graduation.

Thesis Committee:

Tori Forbes, Thesis Supervisor

Edward Gillan

Sarah Larsen

To Neomal,

The most amazing husband

ACKNOWLEDGEMENTS

It is with great respect and honor that I would like to thank my advisor, Dr. Tori Forbes for all the support and guidance rendered to me during the completion of my dissertation and providing me the opportunity to explore a new area of chemistry. Thank you Dr. Forbes, for being the best advisor ever! I would like to thank College of Liberal Arts and Sciences, The University of Iowa for funding this work. A special thank goes to Dr. Daniel Unruh for the guidance given to me in solving crystal structures and all Forbes group members, Josh, Jacob, Mellissa etc. who were there with me during my stay in The University of Iowa.

I am very grateful to Prof. Sarah Larsen and Prof. Ed Gillan for being in my Thesis Committee and for their extensive support in all the revisions and discussions. Special thanks to Prof. Ed Gillan and his group members, The University of Iowa, for the use of FT-IR instrument. I would like to extend my heart felt gratitude to all my teachers whom I met during my life, especially the faculty at the Department of Chemistry, University of Sri Jayewardenepura, Sri Lanka, for all the guidance given to me in becoming the person who I am today. Last but not the least I wish to extend my gratitude to my husband and my mother inclusive of other family members for their love and courage given to me in making this journey a success.

ABSTRACT

Hydrolysis products of aluminum that exist in aqueous solutions play an important role in controlling the fate and transport of contaminants and are also used for coagulants to purification of wastewater streams. Adsorption of contaminants such as heavy metals and organics are widely recognized, but the molecular level understanding of the mechanism of action has not been clearly defined. In this research we present the crystallization, structural characterization and chemical characterization of three novel Keggin-type aluminum polycations including $((Al(IDA)H_2O)_2(Al_{30}O_8(OH)_{60}(H_2O)_{22})(2,6\ NDS)_4(SO_4)_2Cl_4(H_2O)_{40})$ (**Al_{32}-IDA**), $[(Cu(H_2O)_2(\mu_2\text{-}OH)_2)_2(Al_2(\mu_4\text{-}O)_8(Al_{28}(\mu_2\text{-}OH)_{50}(\mu_3\text{-}OH)_6(H_2O)_{26}(2,6\text{-}NDS)_9(H_2O)_{52}]$**-($CuAl_{30}$)** and $[(Zn(NTA)H_2O)_2(Al(NTA)(\mu_2\text{-}OH)_2)_2(Al_{30}(\mu_2\text{-}OH)_{54}(\mu_3\text{-}OH)_6(\mu_4\text{-}O)_8(H_2O)_{20}(2,6\text{-}NDS)_5(H_2O)_{64}]$**- ($ZnAl_{32}$)** where IDA = iminodiacetic acid, NTA- Nitrilotriacetic acid, and 2,6 NDS = 2,6 napthalene disulfonate. These compounds are the first ever reported Keggin-type aluminum species that have been functionalized with organics and heavy metal cations. Structural characterization of these compounds was done by means of single crystal X-ray diffraction along with FTIR, TGA, SEM/EDS and PXRD techniques for chemical characterization. This study provides more insight into the coagulation process and can be employed in developing optimized coagulants for enhanced water purification.

TABLE OF CONTENTS

LIST OF TABLES

Table

LIST OF FIGURES

Figure

LIST OF ABBREVIATIONS

IDA: Iminodiacetic acid

NTA: Nitrilotriacetic acid

2,6-NDS : 2,6 Naphthalene Disulfonate

HEIDI: Hydroxyethyliminodiacetic acid

H_5hpdta: hydroxypropanediaminotetraacetic acid

PACl : Polyaluminum chloride

PXRD: Powder X-ray Diffraction

FT-IR: Fourier Transform Infra-red Spectroscopy

SEM: Scanning Electron Microscopy

EDS/EDX: Energy Dispersive X-ray Spectroscopy

TGA: Thermo gravimetric Analysis

EPR: Electron Paramagnetic Resonance Spectroscopy

DFT: Density Functional Theory

CHAPTER 1

INTRODUCTION

1.1 Significance of Aluminum in the Environmental systems

Aluminum is the third most abundant chemical element in the earth's crust with a natural abundance of 8.3% by weight. Due to its high reactivity with oxygen, aluminum never exists as a pure element in the environment and instead it is found mostly in minerals clays, aluminosilicates and bauxites.[1] Although aluminum as an element, is abundant in the environment, its natural cycling throughout soils, waters and living biomass is still poorly understood.[2]A schematic representation of the aluminum cycle is shown in Figure 1.1 which is proposed by Driscoll and Schecher.[2]

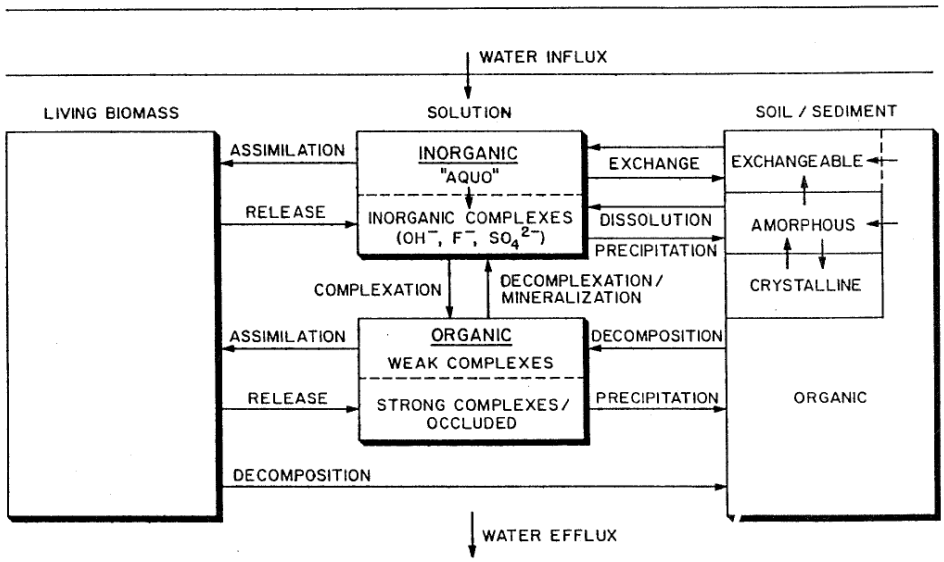

Figure 1.1 Schematic representation of Aluminum cycle[2]

Soil minerals are the primary source of aluminum to aqueous and biological environments.[2] Aluminum enters into the soil via weathering of aluminosilicates, organic acid dissolution, and neutral hydrolysis. Both amorphous and crystalline aluminum compounds exist in the soils and sometimes organic matter is bound with them. These aluminum species can exchange into the aqueous media through dissolution and decomposition of the soil aluminum materials. Within the aqueous environment aluminum can exist as hydroxides, fluorides, sulfates, phosphates, bicarbonates, and silicates. These aqueous aluminum forms can either exchange back in to soils or it can assimilate in living biomass. The aqueous inorganic aluminum species can form strong and weak complexes with organic substances as well. Aluminum in living biomass can enter back in to soils as complexed species via decomposition.

Aluminum is an amphoteric metal and in natural systems tends to undergo hydrolysis and form a myriad of aluminum species in the environment. Determining the exact nature of aqueous aluminum species present in natural systems is crucial for a complete understanding of the fate and transport of aluminum. This requires a molecular level understanding of the formation mechanism of these species including aggregation, nucleation, olation reactions, formation of soluble precursors, and transformations of amorphous or crystalline phases.[3] Even though the hydrolysis and polymerization of Al^{3+} in aqueous solutions have been studied for a long time, the mechanisms are not clearly defined. [4-9]

Aqueous Al^{3+} undergoes complex physicochemical reactions such as hydrolysis, polymerization, adsorption, and complexation on the interfaces of mineral/water.[4] Al^{3+} cation forms a hexa coordinated aqua complex, $[Al(H_2O)_6]^{3+}$ in water. Depending on the

pH of the medium it can form $[Al(OH)_h(OH_2)_{6-h}]^{(3-h)+}$ aquaoxyhydroxo species.[10] These species can undergo condensation reactions by eliminating a molecule of water to produce polymeric species. These are called olation reactions and are usually fast due to the lability of water molecules.[5]

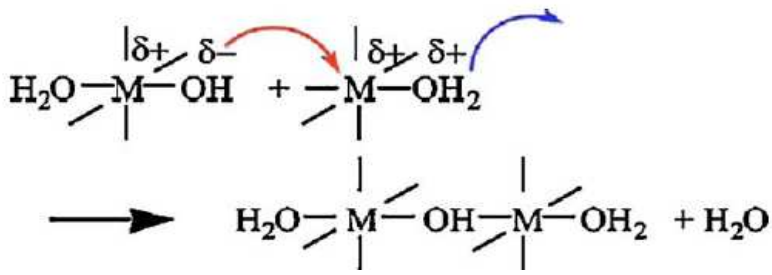

Figure 1.2 Olation Mechanism[5]

On the other hand oxyhydroxo compounds with no water molecules in the coordination sphere have to undergo a two-step process for hydrolysis. These reactions are called oxolation reactions and they create an oxo bridge leading to the formation of a water molecule. Both monomeric and polymeric aluminum species interact with the surrounding geologic media and can adsorb on to clays, other minerals, and alumina, with interactions that are considerably strong.[11] In addition, these species can complex with organic compounds in the environment and several studies indicate that these organic aluminums appear to be more toxic than the free aluminum compounds.[12]

1.2 Aluminum Species found in Solutions

To gain a more complete understanding of the hydrolysis of aluminum in aqueous systems, identifying and understanding the species present in solution is imperative.

Aluminum is considered as a hard Lewis acid and it coordinates well with hard Lewis bases such as oxide, hydroxide and fluoride[13]. The common monomeric forms that are found in aqueous solutions are $[Al(H_2O)_6]^{3+}$ and $[AlOH(H_2O)_5]^{2+}$ like hydrolysis species that exist at very low pH values, usually less than pH 3. These monomeric forms have been identified by ^{27}Al-NMR in solution as well as through potentiometric studies[14]. Dimeric species have also been identified both by potentiometric studies and by the crystallization of $Al_2(OH)_2(SeO_4)_2(H_2O)_{10}$ (s) which contains the unit, $(H_2O)_4Al(\mu\text{-}OH)_2Al(H_2O)_4$.[15] It is believed that planar aluminum trimers also exist in aqueous solutions[13] and are most likely the primary building block of larger nanoclusters. The uncomplexed trimeric species has not been structurally characterized; however, a citrate coordinated aluminum trimer has been synthesized by Feng et. al. in 1990[16] that contains different linkages than those expected for the planar species. Tetrameric aluminum species have not been detected by potentiometric or NMR studies but have been crystallized from a concentrated $AlBr_3$ solution.[17]

The dominant multimeric species found in solutions at pH 3.5 -4.5 is the $[Al_{13}O_4(OH)_{24}(H_2O)_{12}{}^{7+}]$ (ε-Al_{13}) tridecamer. These molecules are synthesized by titrating a relatively concentrated aluminum solution with a base at a hydrolysis ratio (OH^-/Al^{3+}) that is maintained between 2.1-2.5. Structural characterization of this polycation was performed by Johannson in 1960 and it was identified as a Keggin-type molecule, which contains a central tetrahedral unit, $Al(O)_4$ surrounded by twelve $[AlOH(H_2O)_5]^{2+}$ octahedral units. The structure contains four planar trimeric groups which are interconnected through the tetrahedral polyhedron. Presence of the two polyhedra can be identified in solution by ^{27}Al-NMR spectra as two distinct peaks. A

narrow peak at +62.5 ppm in the spectrum corresponds to the highly symmetrical tetrahedral unit whereas the broad peak at +10 ppm is due to the octahedral aluminum sites.[13] After its structural characterization, the Al_{13} molecule has been found in, rivers affected by acid mine drainage[18], soils[19], cultivated plants[13], deodorants, and as a coagulant in water purification[3].

Aging of Al_{13} aqueous solutions produces δ-Al_{13} clusters which then assemble together to yield much larger aluminum clusters. The Al_{30} polyoxocation is one such polynuclear aluminum species identified by Rowsell and Nazar[20] after heating a partially hydrolyzed aluminum solution at 80-90 ^{0}C for a couple of days. Keggin-type clusters can be identified by ^{27}Al-NMR. (Figure 1.3) NMR spectrum of these species, contains a broad peak centered around 0 ppm which is associated with the octahedrally coordinated aluminum atom. The peak corresponding to the tetrahedral site appears down field and its shift is characteristic for different polymeric species. Position of this peak allows the identification of the Keggin as the peaks are at 62.9, 64.5 and 71 ppm for ε-Al_{13}, δ-Al_{13}, and $Al_{30,}$ respectively.[7, 21] However the presence of these species cannot completely be determined by ^{27}Al-NMR as certain species cause broadening of the baseline by quadrupolar relaxation in room-temperature solutions and may be completely overlooked without additional characterization.

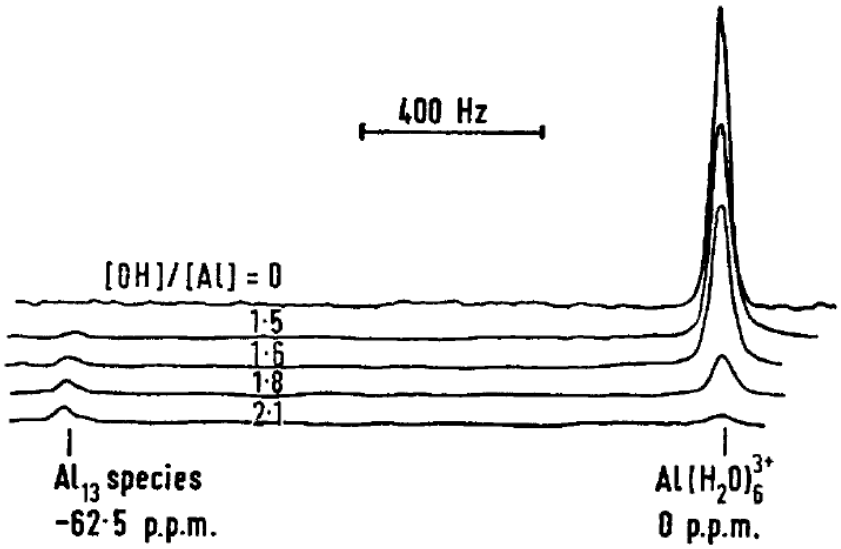

Figure 1.3 ^{27}Al Spectra at 23.45 MHz of 0.2 M aluminium solutions at various degrees of hydrolysis[12]

1.3 Structural Characteristics of the Keggin Isomers

The Baker-Figgis-Keggin or Keggin clusters is a common topology for polyoxometallate species that contain a central tetrahedral aluminum unit which is surrounded by twelve octahedral units. This can be formed as five different isomers from α to ε as shown in Figure 1.4. The predominant species in partially hydrolyzed aluminum species is the ε-Al_{13} isomer and it contains four $[Al_3(\mu_2\text{-}OH)_6(H_2O)_3]$ trimers that are connected together by edge-sharing hydroxyl groups. Rotation of one of these trimers by 60° results in shared hydroxyl vertices and it leads to the formation of δ- Al_{13} isomer. Each of the trimers present in the structure continues to rotate in the formation of the γ-, β-, and α-isomers and the α-isomer contains three rotated trimers linked through vertex sharing hydroxyl groups. With prolonged aging the ε can easily be converted to the δ form but the mechanism of conversion still remains unknown.

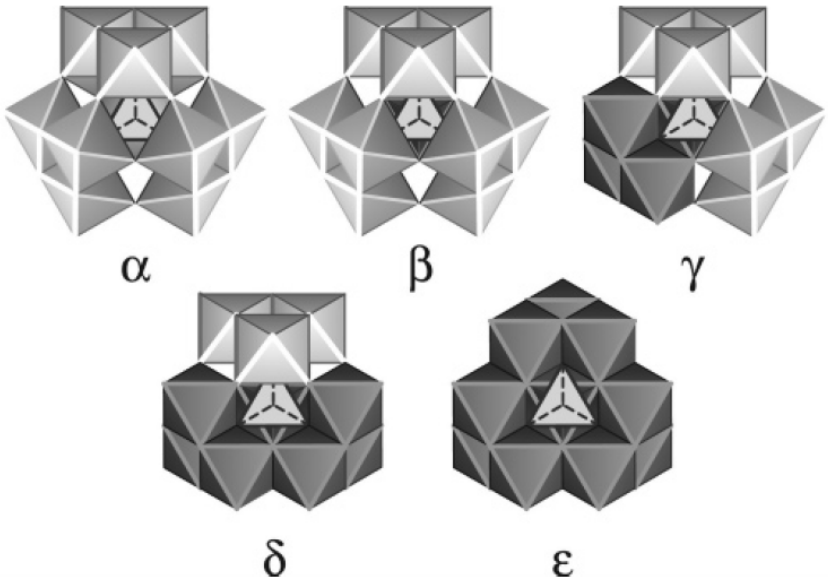

Figure 1.4 Polyhedral representations of Baker-Figgis-Keggin structures[13]

Out of all these Keggin-type Al_{13} isomers, only the δ- and ε- isomers have been crystallized and structurally characterized.[15] The δ-Al_{13} form can polymerize itself leading to the formation of larger aluminum polycations. Al_{30}, Al_{32} and the novel cluster Al_{26} are examples of such polymerized species. Al_{30} is a Keggin-type polycation which contains two δ-Al_{13} units connected together via four octahedrally coordinated aluminum atoms. This molecule has been synthesized and structurally characterized by three individual research groups including our own.[20, 22, 23] S-Al_{32} is the largest aluminum polycation known to date and it contains a sulfate group attached to the exterior of the cluster.[24] In addition to that we were able to synthesize Al_{26} aluminum polycation which is a novel compound containing two δ-Al_{13} units connected through vertex sharing of hydroxyl groups.[23] This molecule can be considered as an intermediate product in the polymerization of Al_{30}. Each of these aluminum polycations is shown in Figure 1.5.

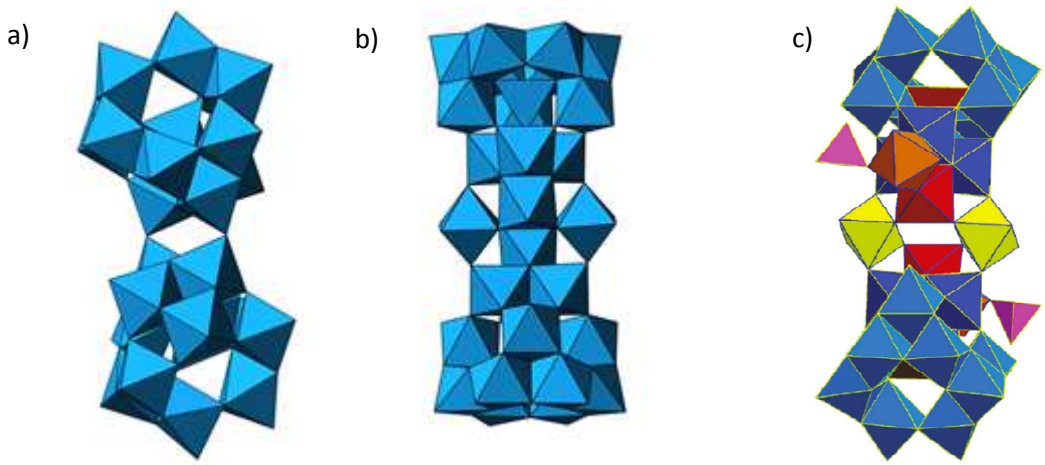

Figure 1.5 Keggin-type large aluminum polycations (a) Al_{26} [29](b) Al_{30}[29] (c) S-Al_{32}[30]

1.4 Importance of Polynuclear Aluminum Species in Environmental systems

Increasing the concentration of aluminum in natural waters and soils due to acid deposition and acid-mine drainage has been reported to be toxic to fish, other marine organisms and plants. Aluminum's behavior in complex ecosystems or living organisms, its bioavailability, toxicity and the reactivity depends mainly on the chemical forms in which it exists. It has been found that in the polynuclear hydroxo-aluminum complexes are much more toxic than the monomeric species or the hexahydrated ions.[4, 18, 19]
The environmental relevance of the aluminum species is also highlighted with contaminant transport, as aluminum sols have shown to be a facilitator in the transportation of heavy metal cations out of mining areas[18]. Heavy metal cations can bind to the sols and forms complexes, but they remain soluble in the mining areas due to the acidity in the environment. Soon after they leave the mines and contact with the natural water bodies, the cations attached aluminum complexes, fall out of solution and form flocculants at relatively increased pH levels in the natural water bodies.[25] A similar kind

of process is used in drinking water purification where heavy metals and other contaminants are removed by aluminum compounds via precipitation and filtration.[26]

1.5 Supramolecular Approach to Crystallization

The structural characterization of aluminum hydrolysis products, including polynuclear species, is important for a molecular level understanding of aluminum cycling, contaminant transport, and water purification processes. Crystallization of these materials is difficult as proven by the fact that over the past 50 years only a handful of aluminum clusters have been isolated.[7,17,20-22,27-29]Most of these clusters are isolated by the addition of sulfate or selenate anions which is essential for the crystallization process. Armstrong et al, in 2011 reported that the enthalpy of formation from the oxides of the ε-Al_{13} cluster crystallized with sulfate or selenate as -1744.55 and -1189.01 kJ/mol, respectively, suggesting stability of these compounds.[30] Although aluminum Keggin-type clusters are synthesized in the presence of sufate or selenate salts, only a fewer number of crystals had been isolated. This suggests the requirement of a different approach for crystallization. The size, charge, and prevalence of hydrogen bonding within these clusters, indicates that a supramolecular approach may be warranted.

Most of the polynuclear aluminum complexes were isolated in the presence of simple anions such as SO_4^{2-}, SeO_4^{2-} and Cl^-. These anions assist in the maintenance of the electroneutrality of the large aluminum clusters with a large cationic charge on them. In the synthesis of Keggin-type aluminum compounds a supramolecular approach has also been applied for crystallization.[21, 31] One such example is the use of a complex polyanion *p*-sulfonatocalix[4]arene in the isolation of ε-Al_{13} cluster in the presence of sodium-18-

crown-6 molecule. The structure is linked through by hydrogen bonding interactions between the sulfonate functional group and the aluminum polycation, but supramolecular interactions like π-π interactions and electrostatics also play a major role. Similarly cucurbit[6]uril has also been used as a co-precipitating agent in the synthesis of ε-Al_{13} and Al_{30} where nitrate ions are present in the structure for charge balancing.

One of the major results from the research presented herein, indicates that the supramolecular interactions between 2,6 Naphthalene disulfonate (2,6 NDS) is novel and successful co-precipitating in synthesizing polynuclear aluminum clusters. Addition of relatively dilute solutions of 2,6 NDS into reaction mixtures containing partially hydrolyzed aluminum assists in the crystallization of many polynuclear aluminum clusters. The 2, 6-NDS molecule has proven to be quite flexible as small changes in the concentration of the 2, 6-NDS anion resulted in higher levels of control over the crystallization of Keggin-type clusters.[23]The use of 2,6-NDS as a supramolecular linker resulted in the synthesis of δ-Al_{13}, Al_{30} and a novel cluster Al_{26}, which is identified as an intermediate in the formation of Al_{30} polycation.

1.6 Overview of the Research

The main focus of my Masters research project was to gain a molecular level understanding of the adsorption of small organic molecules and heavy metal cations on to the polynuclear aluminum clusters. The synthesis, structural and chemical characterization of the compound $(Al(IDA)H_2O)_2(Al_{30}O_8(OH)_{60}(H_2O)_{22})$(2,6 NDS)$_4(SO_4)_2Cl_4(H_2O)_{40}$ - **Al_{32}-IDA,** in which two molecules of Iminodiacetic acid (IDA) are bonded to the exterior of the Al_{32} cluster is reported. Additionally, this dissertation

reports two other structures with Cu^{2+} and Zn^{2+} attached on to the surface of polynuclear aluminum complexes including $(Cu(H_2O)_2(\mu_2\text{-}OH)_2)_2(Al_2(\mu_4\text{-}O)_8(Al_{28}(\mu_2\text{-}OH)_{50}(\mu_3\text{-}OH)_6(H_2O)_{26}(2,6\text{-}NDS)_9(H_2O)_{52}$ **- $CuAl_{30}$** and $(Zn(NTA)H_2O)_2(Al(NTA)(\mu_2\text{-}OH)_2)_2(Al_{30}(\mu_2\text{-}OH)_{54}(\mu_3\text{-}OH)_6(\mu_4\text{-}O)_8(H_2O)_{20}(2,6\text{-}NDS)_5(H_2O)_{64}$ – **$ZnAl_{32}$-NTA.** The syntheses of these compounds require the presence of a co-precipitating agent. The co-precipitating agent that was used in this study was the sodium salt of 2,6 – Naphthalene disulfonic acid. (Figure 1.6)

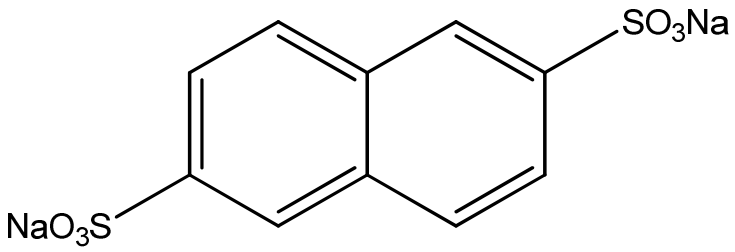

Figure 1.6 Disodium 2,6-naphthalene disulfonate

Principle characterization method for these compounds was single crystal X-ray diffraction. However for additional characterization PXRD, TGA, SEM/EDS and FTIR techniques were used. In addition, mass-spectrometry, small angle X-ray scattering (SAXS) and Pair distribution function (PDF) analysis studies can be used to gain further insight into it. In the forthcoming chapters, the approach towards the crystallization process, and the characterization techniques along with a brief review of the importance of these clusters in an environmental stand point and the future prospects of this research will be described.

CHAPTER 2

MATERIALS AND METHODS

The three cluster compounds, **Al_{32}-IDA**, **$CuAl_{30}$** and **$ZnAl_{32}$** described in this dissertation were synthesized by means of solvothermal synthesis employing Teflon lined Parr bombs with an internal volume of 23 mL. In the preparation of all of these materials the presence of a complexing agent is sometimes used to trap the metal cation in solution, preventing uncontrolled hydrolysis and the formation of insoluble hydroxides. In some cases the complex of cations along with an organic ligand, binds to the cluster via hydroxyl bonds. Compounds shown in Figure 2.1 are the organics that were used in preparation of these materials. Herein the synthesis of the above three materials and techniques used for chemical characterization is described.

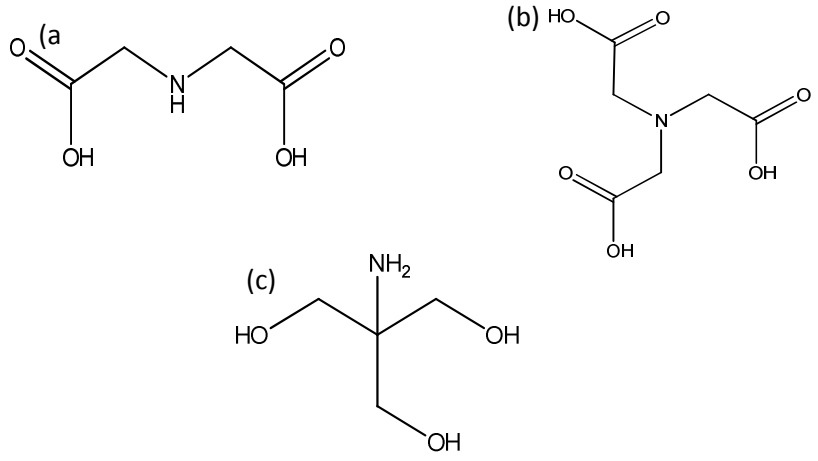

Figure 2.1 Structures of (a) Iminodiacetic acid (IDA) (b) Nitrilotriacetic acid (NTA) (c) Trizma base

2.1 Solvothermal Synthesis

Solvothermal synthesis is a method that is being employed in the synthesis of crystalline materials. This is very much similar to hydrothermal synthesis except organic solvents are preferred over water as the solvent. However in my syntheses the reactants were dissolved in water and placed in a Teflon-lined cup which was sealed in a stainless steel Parr reaction vessel. In this experimental setup, water acts as both a pressure transmitting medium as well as a solvent. The bombs that were used in the syntheses of the above compounds had an internal volume of 23 mL. The reactants were heated at 80 ^{0}C for 24 hours in a gravimetric oven. The contents were allowed to cool to room temperature before adding 2,6- Naphthalene disulfonate which acts as the co-precipitating agent thereby inducing crystallization.

The crystals are usually formed at the bottom of the vials and they were scraped off and transferred to a glass slide using a glass transfer pipet. The contents in the glass slide were examined under a microscope and good quality crystals were isolated for further studies.

2.2 Single Crystal X-Ray Diffraction

Single X-ray diffraction can be considered as the primary technique for the characterization of highly-crystalline materials. Determining a crystal structure involves the identification of the precise spatial arrangement of all of the atoms in a chemical compound. Successful structure determination provides information about connectivity, conformation, and accurate bond lengths and angles.[32] Monochromatic radiation is necessary for the structure determination. For structure determination monochormatic Kα

radiation is preferred and a monochromator is used to remove both the background (bremsstrahlung) and the smaller K_β peak. A crystal is mounted on a cryo-loop by a viscous oil called Infinium and placed on the gonionmeter head. The crystal is centered in the X-ray beam, exposed to monochromatic radiation, and coherent X-ray beams are diffracted off the crystalline lattice creating the diffraction pattern.

When there's constructive interference, Bragg's Law can be used to explain the planes in a crystal. Bragg's Law is given as $n\lambda = 2d \sin\theta$ where, n is the order of reflection, λ is the wavelength of the monochromatic X-ray radiation, d is the lattice spacing and θ is the angle of incidence or the Bragg angle. The type, the arrangement and the amount of different types of atoms present in the crystal determines the intensity of the reflections that are being observed.[35]

There are a number of factors which can affect the intensity of X-rays in the diffraction pattern. Structure factor is one of those which solely depends upon the crystal structure.[33]

$$F(hkl) = \Sigma f_i \exp [2\pi i (hx_j + ky_j + lz_j)]$$

In addition to these the diffraction intensity can further be affected by absorption, polarization, temperature, multiplicity, and the Lorentz factor.

2.3 Structure Determination

The crystals were separated from the mother liquor and with the aid of Infiniuim oil they were mounted on a Nonius KappaCCD single crystal diffractometer with Mo Kα radiation ($\lambda = 0.7107$ Å) and a low temperature cryostat. Data collection, cell refinement, data reduction and absorption corrections were performed using Collect[34] and

APEXII[35] software respectively. Absorption corrections were done using SADABS[36] program contained within APEXII software. Structure solution was done by means of direct methods and the refinement was done on the basis of F^2 for all unique data using the Bruker SHELXTL version 6.10 programs[36]. Atomic scattering factors for each atom were obtained from International Tables of X-ray Crystallography.[37]

Accurate determination of the location of hydrogen atoms using X-ray diffraction is difficult because of their low scattering powers. Therefore certain measures are needed to be taken into account when modeling hydrogen atoms. XL, which is the structure refinement part of SHELXTL software, provides options for the placement and refining of hydrogen atoms using HFIX and AFIX commands. Therefore hydrogen atoms associated with the naphthalene groups were added using HFIX command. When bond lengths and angles of a compound refine far from their chemically sensible values we can restrain those using DFIX command in XL. The DFIX command can also be used to model disorder of individual atoms, thus some of the disordered sulfur and oxygen atoms associated with the 2,6 NDS molecules were modeled as split sites and the naphthalene rings were refined as rigid groups using the DFIX command.

Disorder can be quite significant with the crystallization of polynuclear aluminum species, particularly for solvent molecules. In crystallization, chemical compounds crystallize along with the solvent molecules that were used in the synthesis. These solvent molecules occupy large void spaces associated with clusters and are in constant motion creating diffusion in residual electron density map of the structure model. This smearing out of electron density affects the proper refinement of the structure. SQUEEZE command in the PLATON software is designed to deal with the solvent disorders and

allows for a better refinement of the structures. Therefore during the structural refinement of all the clusters, the disordered solvent (H_2O) was modeled using the SQUEEZE command in the Platon software[38].

2.4 Powder X-ray Diffraction

Many compounds are conveniently prepared as polycrystalline materials and hence powder X-ray diffraction is helpful for phase identification and purity.[39] The prepared materials were examined by powder X-ray diffraction using a Bruker D5000 powder X-ray diffractometer equipped with a Bruker LynxEye solid state detector. Approximately 50 mg of the sample was ground into a slurry using acetone as the solvent and transferred in to a glass plate using a glass pipette. Scans from 10^0 to 70^0 with a step size of 0.05^0 per second were collected to investigate the purity of the prepared crystalline material used for single-crystal X-ray diffraction studies.

2.5 Scanning Electron Microscopy[40] with Energy Dispersive Spectroscopy[41]

Knowledge of the physical nature of the surfaces that we are dealing with is important in all areas of science. In scanning electron microscopy an electron gun is used to generate thermionic electrons. When obtaining an image, the solid surface is rastered with the electron beam. Several types of signals are produced in this technique, but the most important are the back scattered and secondary electrons which provides the basis for this technique.

Energy Dispersive X-Ray Spectroscopy (EDX/EDS) is a useful technique in elemental mapping. In this technique, characteristic X-rays are being used. The generation of characteristic X-rays initiates with the collision of an electron beam with a

sample which results in the ejection of an electron from inner shells creating a vacancy. Then an upper shell electron drops off to fill the vacancy generating X-rays with energy similar to the energy difference in the two shells. The nomenclature for the generation of X-rays depends on the initial shell where the vacancy is created. Thus the emissions are named K, L, and M etc.

For the purpose of determining the size, morphology, and the elemental composition of the crystalline material Hitachi-S3400N Scanning Electron Microscope equipped with Electron Dispersive Spectroscopy was used. Crystals were separated from the mother liquor and mounted on a SEM stub with a double-sided carbon tape on it. The operating voltage and the emission current was 15.0 kV and 80-120 μA respectively.

2.6 Thermogravimetric Analysis

Thermogravimetry measures the change in mass of a substance as a function of temperature and/or time.[34] In this technique, a sample of a known weight is heated at a constant rate. Weight losses are observed at different temperatures depending on the material that correspond to processes such as water loss, decomposition, and oxidation. This analysis was performed on the synthesized materials using a TA instruments TGA Q500. Approximately 15-20 mg of the finely ground sample was taken and it was heated in the presence of air from 25 ^{0}C to 600 ^{0}C at a ramp rate of 5 ^{0}C/min.

2.7 Fourier Transform Infrared Spectroscopy

Infra-red spectroscopy is useful in the identification of lighter elements and the chemical bonds associated with them, that in some cases cannot be accurately assigned

using single crystal X-ray diffraction studies. The interaction of IR radiation with chemical bonds results in vibrational excitation of the molecules in the sample. Thus this technique is capable of providing evidence for the presence of various functional groups. Infrared spectra for the synthesized materials were obtained using a Nicolet Nexus FT-IR Spectrometer. A quantity of the sample was mixed with approximately ten times potassium bromide and the pellets made were run from 500-4000 cm^{-1}. Blank subtractions were also done using pure KBr pellets.

2.8 Bond Valence Calculations[42, 43]

The chemical bond is an empirical concept that is used in chemistry that helps understand the relationship between two atoms. When considering a chemical bond the electrons are shared between the atoms importing it some energy which is called the bond strength. The bond strength and the bond distance have an inverse relationship between them. The bond model was brought forward based on Pauling's five principle rules of crystal chemistry which is used to describe complex ionic structures. The idea of the bond strength was thus inspired as the experimental bond valence which can easily be calculated by the following simple mathematical relationship.

$$s = \exp((R_0 - R)/B) \text{ and } s = (R/R_0)^{-N}$$

where, s is the experimental bond valence, R is the bond distance between two atoms, R_0 and B are determined from experimental data obtained for well-defined crystal structures. B is usually 37 pm for most of the structures and N varies from 4 to 6 depending on the compound.

Since the scattering in X-ray diffraction analysis depends on the electron density around an atom, hydrogen atom can be considered as a poor scatterer. Thus bond valence analysis performed on oxygen atoms helps us understand the location and bonding of hydrogen atoms. In this research bond valence calculations were used in order to determine whether the ligands based on oxygen are O^{2-}, OH^{-} or H_2O. The bond valence sum of an oxygen atom needs to be approximately 2 vu (vu=valence units), where any additional hydrogen bonding to oxygen has to be less than that. Generally when the bond valence sum of O is less than 0.5 vu, it's considered as a H_2O molecule and if it is between 0.5 – 1.5 it's considered as a OH. In addition to that, this analysis can be used to determine the oxidation state of the metal. The bond valence tables are included in the Appendix.

CHAPTER 3

THE STRUCTURAL CHARACTERIZATION OF AN ALUMINUM POLYCATION IN THE PRESENCE OF IMINODIACETIC ACID: IMPLICATIONS FOR THE ADSORPTION OF NATURAL ORGANIC MATTER ON COLLOIDAL SPECIES

3.1 Introduction

Organic pollutants in drinking water have become a crucial problem to humans and other organisms as most of the compounds are carcinogenic.[44] Halogenated and polycyclic aromatic hydrocarbons (PAH) are among the most common organic pollutants that enter into the environment via petroleum byproducts, pesticides and herbicides. Use of pharmaceuticals and personal care products has become a major source of contamination of water bodies as these compounds are resistant to degradation and treatment processes.[45] To remove these pollutants from the water\column, requires a variety of physical, chemical and biological treatments.[46] Even though the primary and secondary treatment processes are effective in removing some organics many are resistant. Treatments such as ozonation and reverse osmosis are much more effective but at the same time they substantially increase the cost of the treatment. Thus optimizing the primary and secondary treatment methods could be beneficial in the removal of these contaminants from waste waters.

Removing organic contaminants with the aid of metal salts such as Al^{3+} and Fe^{3+} by coagulation and flocculation during secondary water treatment is currently being used in many treatment facilities. It could be optimized to target specific organic pollutants if

the mechanisms of removal were better understood. Adding salts into wastewaters leads to the formation of metal hydrolysis products which includes soluble polynuclear clusters and larger colloidal species and they aggregate and precipitate into amorphous flocs. Heterocoagulation, sweep flocculation and adsorption processes are the main stream methods of removing contaminants.[44] Most of the hydrolysis products are cationic which can interact with negative impurities which then facilitate the coagulation process. Positively charged aluminum oxyhydroxide colloids adsorb on to larger impurities such as humic acid and precipitate by neutralizing their charge. This process is called the heterocoagulation. Sweep flocculation is another mechanism which removes the contaminants by enmeshing them in the aluminum clusters which are then removed by precipitation. However the removal of small organics from the waste waters is much more challenging. Usually they are removed via the adsorption to the surface of the colloidal species.[47]

Aluminum sulfate (Alum) and ferric chloride are the traditional coagulants but polyaluminum chlorides (PACl) have become more popular due to their high efficiency.[44] PACl coagulants are mainly composed of, Keggin-type tridecamers ($PACl_{Al13}$) and more recently of large Al_{30} polynuclear clusters ($PACl_{Al30}$)[48], with smaller amount of monomeric and dimeric species had been discovered. These coagulants are much more effective in the removal of small molecular organics, but the nature of the coagulation process still remains unresolved. Therefore the synthesis and structural characterization of these compounds with adsorbed organic molecules are essential in order to gain a molecular level understanding of these processes that are occurring in the environment.

In this study we strive to gain a fundamental understanding of the adsorption of small organic molecules such as Iminodiacetic acid (IDA) on to Keggin-type aluminum clusters in order to expand our knowledge on the role of the aluminum polycations in the coagulation process. IDA acts as a good chealator to the aluminum as it contains carboxylic and amine functional groups which are prominent in dissolved organic carbon and small fulvic acid that are difficult to be removed using coagulants. Herein I report the synthesis , structural characterization and chemical characterization techniques of $((Al(IDA)H_2O)_2(Al_{30}O_8(OH)_{60}(H_2O)_{22})(2,6NDS)_4(SO_4)_2Cl_4(H_2O)_{40})$ (**Al_{32}-IDA**), a Keggin-type aluminum polycation with Iminodiacetic acid bonded to an aluminum atom located in the exterior of the cluster.

3.2 Synthesis of Al_{32}-IDA Cluster $((Al(IDA)H_2O)_2(Al_{30}O_8(OH)_{60}(H_2O)_{22})(2,6\ NDS)_4(SO_4)_2Cl_4(H_2O)_{40})$

A stock solution of the partially hydrolysized aluminum solution known to contain a significant amount of ε-Al_{13} was prepared by heating a 25 mL of 0.25 M $AlCl_3$ (6.25 mmol) solution to 80 ^{0}C in a water bath. This was followed by a drop wise addition of 60 mL of 0.25 M NaOH (6.25 mmol) to a hydrolysis ratio (OH^- / Al^{3+}) of 2.4. Approximately 7 mL of the Al_{13} solution was mixed with 0.0312 g of IDA and the solution was stirred for 20 min until complete dissolution of the IDA. The clear solution was loaded in to a 23-mL Teflon-lined Parr acid digestion vessel and heated in a gravimetic oven at 80 ^{0}C for 24 hrs. The resultant solution was cooled, transferred in to a glass vial and 3 mL of 0.1 M 2, 6 NDS was added to induce crystallization. After aging

for approximately 12 days colorless plate-like crystals were formed which were well suitable for single crystal X-ray diffraction studies.

3.3 Structure Determination

Colorless crystals were isolated from the mother liquor and were mounted on a Bruker Nonius KappaCCD single crystal X-ray diffractometer with monochromatic MoKα radiation (λ = 0.7107 Å) along with a low temperature cryostat. Data collection, refinement and adsorption correction were performed using Collect[34] and APEXII[35], respectively. Important data collection parameters and crystallographic information are given in Table 3.1.

Al_{32}-IDA structure was solved using direct methods and refined using Bruker SHELXTL version 5 systems of programs based on F^2 for all unique data. International Tables of X-ray Crystallography were used to obtain the atomic scattering factors for each atom. This compound crystallizes in the triclinic space group, *P*-1 with a = 13.952(2) Å, b = 16.319(3) Å, c = 23.056(4) Å, α = 93.31(1)°, β = 105.27(1)° and γ = 105.52(1)°. The Al and S atoms were located using direct method solutions and the O and C atoms could be identified in the Fourier maps calculated, following the refinement of the partial-structure models.

Significant structural disorder was associated with the solvent water molecules, disulfonate anions and the iminodiacetic acid chelator. The free rotation of the sulfonate groups along S-C bond in the 2,6-NDS anion, leads to an elongation of the electrons associated with the oxygen atoms, but there were no splitting sites to be found. The sulfate anion (S5) was modeled as a split site with an occupancy of 70% and 30% for S5A and S5B, respectively. IDA molecule also contains disorder and required separation

of some C and O atoms into two sites, with 50% occupancy at each atom. Also the compound contains partially occupied chlorine atoms within the void spaces. The water molecules present in the interstitial sites could not be located due to diffuse electron density. The SQUEEZE command in the PLATON[38] software was used to model the diffuse electron density associated with the solvent molecules. This reduced the R_1 value from 16.75% to 9.16%.

Hydrogen atoms of the naphthalene rings and the carbon atoms of the IDA molecule were placed using a riding model with a fixed C-H distance of 0.93 Å. Due to the high disorder of solvent in the interstitial sites, additional hydrogen bonds could not be found. Selected bond distances and angles are listed in table 3.2.

Table 3.1. Selected Crystallographic Information for $(Al(IDA)H_2O)_2(Al_{30}O_8(OH)_{60}(H_2O)_{22})(2,6\ NDS)_4(SO_4)_2Cl_4(H_2O)_{40}$ (Al_{32}-IDA)

a(Å)	13.952(2)	μ (mm^{-1})	0.422
b (Å)	16.319(3)	F(000)	2038
c (Å)	23.056(4)	Crystal Size (mm)	0.185 x 0.17 x 0.095
α (°)	93.31(1)	Theta range	0.92 to 25.04°
β (°)	105.27(1)	Data collected	-16<h<15, -19<k<19, 0<l<27
γ (°)	105.52(1)	Completeness to theta = 25.04°	99.3%
V ($Å^3$)	4805.1(2)	Reflections collected/unique	16894 / 16894
Z	1	GOF on F^2	0.998
FW($gmol^-$)	4902.5	Final R indices [I> 2σ(I)]	R_1 = 0.0888, wR_2 = 0.2810
Space Group	*P*-1	R indices (all data)	R_1 = 0.1026, wR_2 = 0.3019
ρ_{calc} (g/cm^3)	1.020	Largest diff. peak and hole ($Å^3$)	2.537 and -1.383

Table 3.2 Selected bond distances for the aluminum polycation (Al_{32}-IDA)

Al(1)-O(3)	1.876(4)	Al(9)-O(11)	1.835(3)
Al(1)-O(1)	1.879(4)	Al(9)-O(8)	1.840(3)
Al(1)-O(18)	1.893(3)	Al(9)-O(19)	1.854(3)
Al(1)-O(17)	1.895(3)	Al(9)-O(17)	1.865(3)
Al(1)-O(28)	1.934(4)	Al(9)-O(26)	1.994(4)
Al(1)-O(14)	1.957(3)	Al(9)-O(14)	2.010(3)
Al(2)-O(4)	1.826(3)	Al(10)-O(24)	1.839(4)
Al(2)-O(2)	1.840(4)	Al(10)-O(13)	1.843(4)
Al(2)-O(41)	1.848(3)	Al(10)-O(20)	1.857(4)
Al(2)-O(42)	1.968(3)	Al(10)-O(7)	1.871(4)
Al(2)-O(40)	1.971(4)	Al(10)-O(45)	1.939(4)
Al(2)-O(32)	1.981(3)	Al(10)-O(27)	2.035(3)
Al(3)-O(3)	1.835(3)	Al(11)-O(2)	1.877(3)
Al(3)-O(6)	1.839(4)	Al(11)-O(7)	1.886(4)

Table 3.2 continued.

Al(3)-O(43)	1.871(4)	Al(11)-O(23)	1.885(4)
Al(3)-O(42)	1.934(3)	Al(11)-O(5)	1.888(3)
Al(3)-O(38)	1.951(3)	Al(11)-O(34)	1.927(4)
Al(3)-O(32)	1.982(3)	Al(11)-O(27)	1.957(3)
Al(4)-O(22)	1.835(3)	Al(12)-O(25)	1.835(4)
Al(4)-O(11)	1.840(3)	Al(12)-O(21)	1.841(3)
Al(4)-O(9)	1.859(3)	Al(12)-O(15)[a]	1.857(3)
Al(4)-O(18)	1.870(3)	Al(12)-O(40)	1.919(3)
Al(4)-O(44)	1.915(4)	Al(12)-O(42)	1.940(3)
Al(4)-O(14)	2.068(3)	Al(12)-O(38)	1.966(3)
Al(5)-O(13)	1.850(3)	Al(13)-O(29)	1.841(4)
Al(5)-O(22)	1.858(4)	Al(13)-O(20)	1.852(4)
Al(5)-O(23)	1.863(3)	Al(13)-O(12)	1.866(4)
Al(5)-O(9)	1.875(3)	Al(13)-O(24)	1.866(4)

Table 3.2 continued.

Al(5)-O(37)	1.933(4)	Al(13)-O(46)	1.905(4)
Al(5)-O(27)	2.014(3)	Al(13)-O(10)	2.051(3)
Al(6)-O(8)	1.837(4)	Al(14)-O(14)	1.782(3)
Al(6)-O(16)	1.842(3)	Al(14)-O(27)	1.785(3)
Al(6)-O(12)	1.854(3)	Al(14)-O(10)	1.787(3)
Al(6)-O(19)	1.865(4)	Al(14)-O(32)	1.833(3)
Al(6)-O(36)	1.960(4)		
Al(6)-O(10)	2.026(3)	Al(15)-O(41)[a]	1.890(3)
		Al(15)-O(21)	1.891(3)
Al(7)-O(6)	1.863(4)	Al(15)-O(15)	1.897(4)
Al(7)-O(29)	1.881(4)	Al(15)-O(39)	1.897(3)
Al(7)-O(4)	1.888(3)	Al(15)-O(33)	1.917(4)
Al(7)-O(16)	1.892(3)	Al(15)-O(35)	1.964(4)
Al(7)-O(31)	1.917(4)		
Al(7)-O(10)	1.929(3)	Al(16)-O(43)	1.850(4)

Table 3.2 continued.

		Al(16)-O(25)	1.850(4)
Al(8)-O(5)	1.813(4)	Al(16)-O(48)	1.895(4)
Al(8)-O(1)	1.837(3)	Al(16)-O(47)	1.896(5)
Al(8)-O(39)	1.860(3)	Al(16)-O(30)	1.907(5)
Al(8)-O(38)	1.935(4)	Al(16)-N(1)	2.049(6)
Al(8)-O(40)	1.957(3)		
Al(8)-O(32)	2.009(3)		

Symmetry transformations used to generate equivalent atoms; a)-x+1, -y+1, -z

3.4 Structural Description

Al_{32}-IDA contains the molecule $[(Al(IDA)(H_2O))_2(Al_{30}O_8(OH)_{60}(H_2O)_{22})]^{16+}$ as the cationic species and 2,6 naphthalene disulfonates as counter anions. This is made up of a Keggin-type polyaluminum species which contains a central tetrahedral aluminum atom surrounded by twelve octahedral aluminums. (Figure 3.1) The central aluminum atom is bonded to four oxygen atoms with bond distances varying from 1.782(2) – 1.833(3) Å. The octahedral aluminum atoms are bonded to six other oxygen atoms originating from species such as oxygen atoms, hydroxyl groups and water molecules with bond lengths varying from 1.813(4) – 2.051(3) Å. These twelve aluminum atoms are arranged into four planar $Al_3(\mu_2\text{-}OH)_6(H_2O)_3$ trimers via edge-sharing hydroxyl groups.

Each of these trimers and the tetrahedral aluminum atom collectively form the Al_{13} molecule $[Al(\mu_4\text{-}O_4)Al_{12}(\mu_2\text{-}OH)_{24}(H_2O)12]^{7+}$, via a variety of corner and edge-sharing interactions. This Al_{13} is the primary building block of the polynuclear aluminum species. (Figure 3.1 – area circled in red)

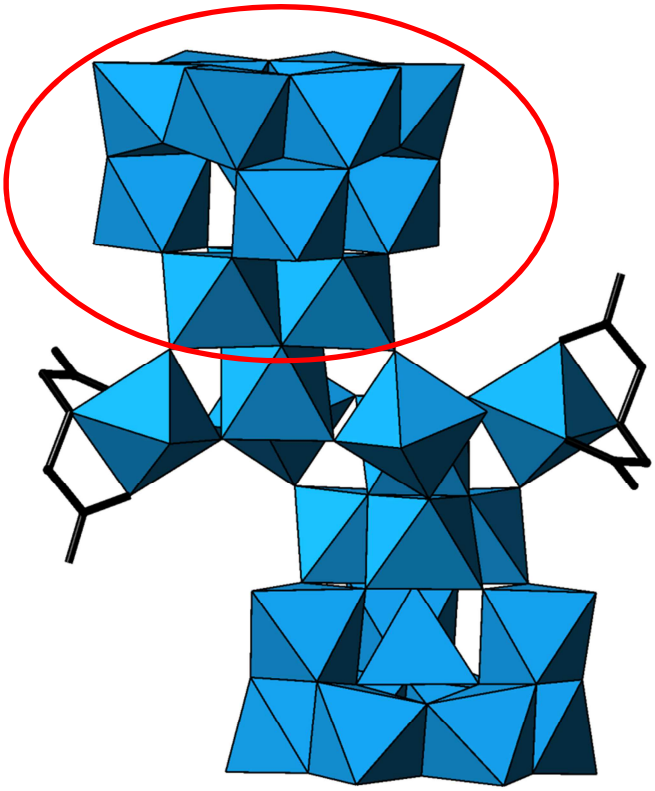

Figure 3.1 Polyhedral representation of Al_{32}-IDA aluminum polycation with two IDA molecules attached to the exterior of the cluster (area circled in red is the δ-Al_{13} Keggin-type moiety) Aluminum- blue, IDA- black.

When ε-Al_{13} containing solutions are aged or gently heated for couple of hours, larger polyaluminum species tend to form. The **Al_{32}-IDA** is one such species which is formed by connecting two δ-Al_{13} moeities through six octahedrally coordinated

aluminum atoms. The two δ-Al_{13} units are directly connected to four of the octahedral aluminums in the middle and the other two are bonded in a bridging- bidentate fashion to the Keggin polynuclear species and each atom is chelated by an IDA molecule. (Figure 3.1) The IDA bonds to the aluminum atoms through oxygen atoms of the carboxylate group and the nitrogen of the amine in a tridentate fashion. This interaction forms a octahedral coordination for the aluminum atoms with Al-O and Al-N bond lengths ranging from 1.850(4) – 2.049(6) Å.

The **Al_{32}-IDA** molecules forms an ordered three-dimensional crystalline structure via hydrogen bonding with the deprotonated disulfonate anions located in the interlayer spacing. (Figure 3.2) Four 2,6-NDS anions per unit cell are stacked vertically in the structure with a distance of 3.4 Å between the naphthalene rings. This distance is within the range to potentially give rise to Van der Waals and π-π interactions between the disulfonates. In addition, hydrogen bonding occurs between the hydrogen atoms of OH and H_2O molecules that are bonded to the aluminum atoms and the oxygen atom of the sulfonate moieties. The larger size, van der Waals interaction, hydrogen bonding and the negative charge helps in the crystallization of the polyaluminum species from the aqueous media.

There are two additional free sulfate molecules per unit cell, available in these structures which can also participate in hydrogen bonding. (Figure 3.2) Discovering these sulfates in the structure was surprising as it was not a starting material in our synthesis. However we observed the breakdown of 2,6 NDS in our own laboratory in the presence of UV light. A sulfonate functional group leaves the naphthalene ring to create an organosulfonate ligand which was confirmed by mass spectrometry. The solutions that

made Al_{32}-IDA crystals were not intentionally exposed to radiation, but they were aged in glass scintillation vials for weeks which may have facilitated the breakdown of the sulfonate moiety. In addition, Szabo-Bardos et al.[49] have observed the photodegradation of organics in the presence of colloidal TiO_2 and therefore we can conclude that the presence of an aluminum polycation may have also lead to the decomposition of the 2,6 NDS anion.

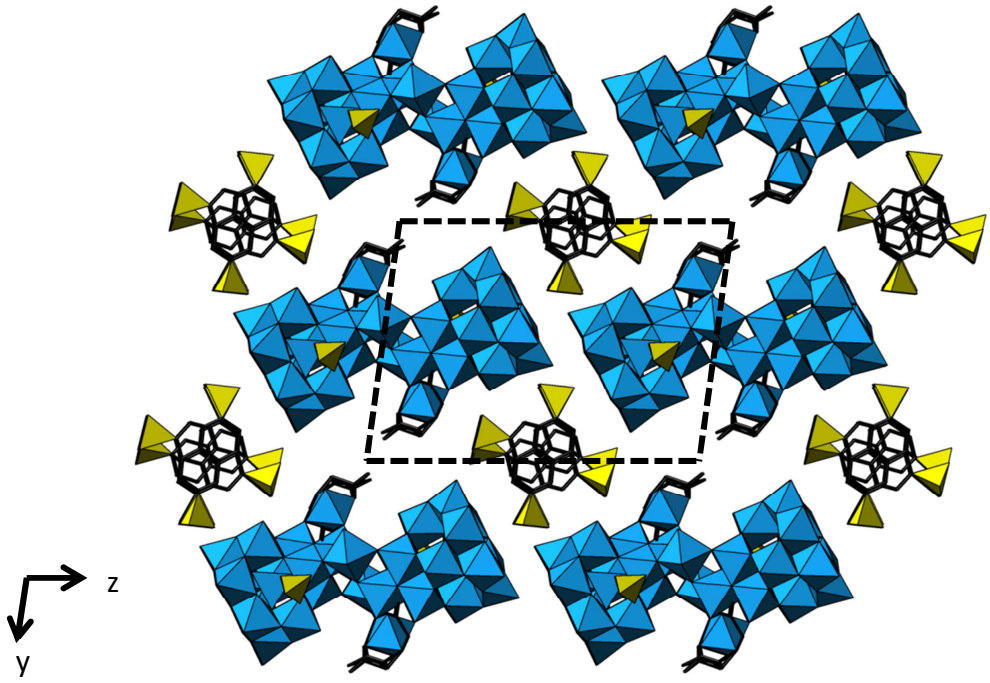

Figure 3.2 Three dimensional network structure of Al_{32}-IDA with 2,6 NDS linking the polynuclear species

The electroneutrality of the overall structure is maintained by chlorine atoms that were also located with partial occupancy. The remainder of the void spaces (1172 $Å^3$) was populated with H_2O molecules.

3.5 Chemical Characterization

3.5.1 Fourier Transform Infrared Spectroscopy

A sample of **Al_{32}-IDA** was subjected to Infrared spectroscopy to confirm the structural components of the compound. (Figure 3.3) An infrared band for the symmetry stretching vibration associated with the AlO_4 species is observed at 777 cm^{-1}. A similar band is observed on the ε-Al_{13} chlorohydrate structure at 780 cm^{-1}.[50] The O-H stretching vibrations are also observed for the octahedrally coordinated aluminum atoms, which appears between 2500-3100 cm^{-1} The O-H stretching peak extends out to about 4000 cm^{-1}, which indicates the presence of water molecules. Stretching bands for C-O, C-N and C=O are observed at 1210, 1330, and 1410 cm^{-1} respectively, and are in correspondence with the previously reported values for the deprotonated IDA molecule.[51] The carbonyl associated with the COOH group for IDA usually occurs at 1715 cm^{-1} and the shift of this peak in our IR indicates that the IDA is definitely deprotonated and complexed to the metal cluster. Even though it was expected to observe the N-H absorption band around 3099 cm^{-1}, the peak is likely hidden by the broad IR band for hydroxyl groups. The IR spectrum of 2,6-NDS as shown in Figure 3.4 is quite complex, because it contains a variety of C-C, C-H, S-O stretching frequencies. These peaks correspond to most of the peaks in the Al_{32}-IDA spectrum. The presence of sufate anion in the compound could not be verified since the vibrational bands for this are very much similar to the peaks that are observed for the sulfonate functional group.

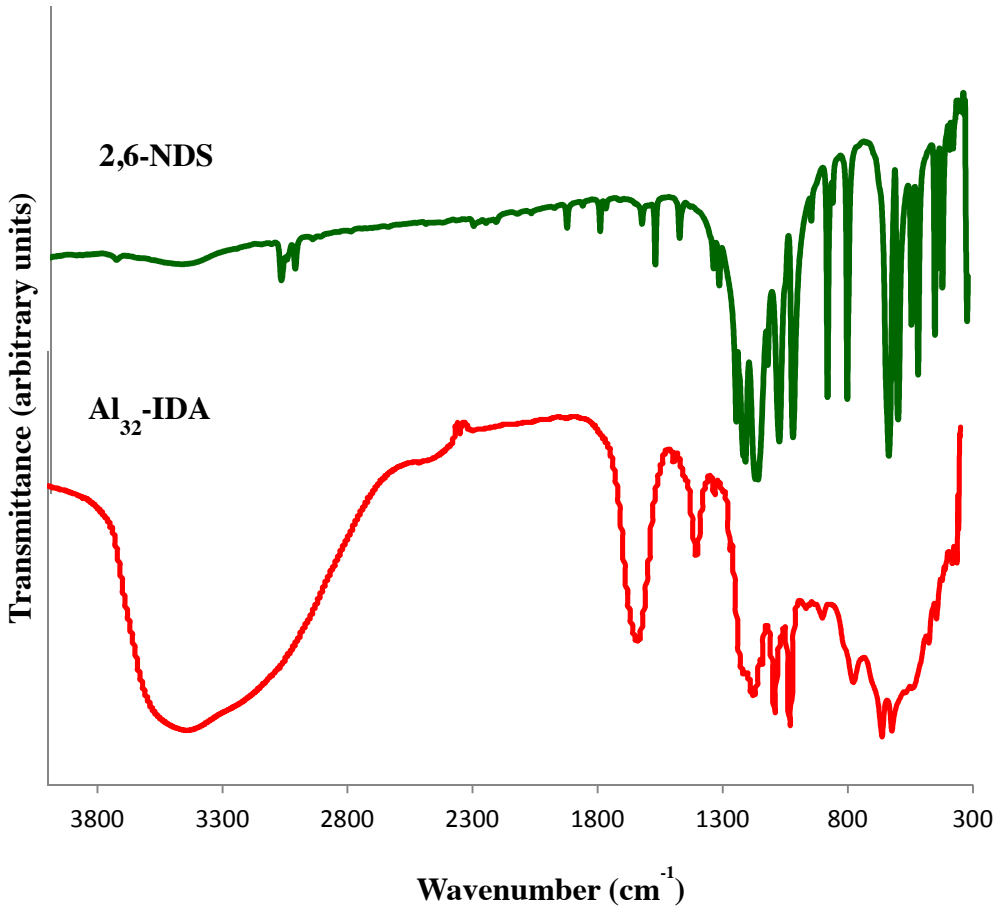

Figure 3.3 Infrared Spectrum of Al_{32}-IDA and 2,6 NDS

3.5.2 Thermogravimetric Analysis

Al_{32}-IDA sample was subjected to thermogravimetric analysis attempting to quantify the number of solvent waters that are present within the structure. (Figure 3.4) The solvent waters are bonded to the cluster through intermolecular hydrogen bonding, thus making the solvents less tightly bound. During the incineration process these waters are more likely to be removed within the temperature range of 80- 120 ^{0}C. The weight loss associated with this is around 14.64% which accounts for 40 molecules of solvent waters per formula unit. Water molecules that are bonded to the aluminum atoms on the

cluster are more likely to be removed around 150-300 ^{0}C. For this particular compound the experimental water loss was about 12.35% where as it was expected to be around 11.431%. This is an expected discrepancy as the loss of materials during an incineration occurs at fairly a wide temperature range. Loss of organics i.e. IDA, from these materials occur around 300-400 ^{0}C with an experimental loss of 8.64%. However according to the calculations based on the formula mass it was about 5.34%. The 2,6 NDS molecules which are considered as rigid stable molecules decompose from 400 -600 ^{0}C liberating CO_2, H_2O and SO_x in the process.

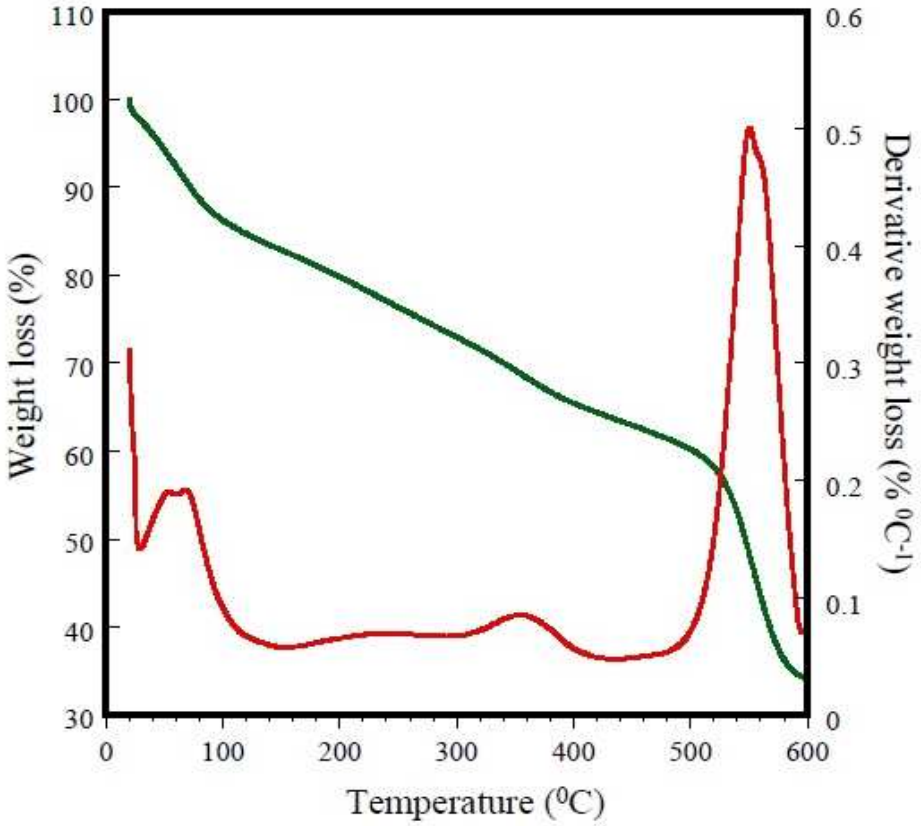

Figure 3.4 Thermogravimetric analysis data plots for Al_{32}-IDA

However this molecule contained 4 groups of Cl^- and 2 groups of SO_4^{2-} which again could be expected to decompose in to gaseous species at this temperature. The theoretical and experimental weight losses match up very closely as they both were about 30%. Weight losses associated with the final product suggests that our final product is most likely to be Al_2O_3.

3.6 Discussion

3.6.1 Coordination of aluminum species with small organic ligands

Several monomeric and dimeric aluminum coordination complexes chelated with organic ligands have previously been identified. These ligands are more often incorporated into the reaction mixtures in order to compensate for the high cationic charge associated with the polynuclear aluminums. Having an organic ligand in the structure not only helps charge balancing but also helps in completing the coordination environment of the peripheral aluminum atoms. In addition to that, it can prevent aggregation and precipitation of the aluminum clusters. Presence of organic ligands can also affect the charge, size and the geometry of the cluster too. Thus a wider variety of interesting compounds can be formed via the incorporation of organic ligands into the synthesis of larger polynuclear compounds.

An interesting ligand coordinated structure is the aluminum dimer with the hydroxyethyliminodiacetic acid (H_3-HEIDI) ligand.[52] In this compound the hydroxyl bridges are being replaced by the ethoxy groups of the HEIDI ligand. Aluminum completes its coordination environment by binding to the oxygen atoms of the carboxylate groups, two ethoxy groups, one water molecule and one imino nitrogen atom.

This was isolated in the presence of $Al(NO_3)_3.9H_2O$ but replacing it with $AlCl_3.6H_2O$ can yield a similar compound with Cl^- as the counter anion.

Attempts have been made in the past to use a variety of carboxylic acids as ligands in the crystallization process of polynuclear aluminum clusters. Nitrilotriacetic acid (NTA) and iminodiacetic acid (IDA) are being extensively used in making these clusters both in the past and the present.[53,54] Other ligands that are reported from past studies are 2-(2'-hydroxyphenyl)-2-benzoxazole[16], citrate[55,56], hydroxypropanediaminotetraacetic acid (H_5hpdta)[57] which led to a considerable number of crystalline materials.

3.6.2 Functionalization of Keggin-type polyaluminum compounds with organics

The Al_{32}-IDA compound gives the first insight into the functionalization of a Keggin-type aluminum compound with a small organic molecule. In the past, aluminum dimers have been functionalized using carboxylates, such as hydroxylethlyiminodiacetic acid (HEIDI), nitrilotriacetic acid (NTA), and IDA. In addition to that large polynuclear species have also been synthesized such as, $[Al_{13}(OH)_{18}(H_2O)_5(HEIDI)_6]^{3+}$ but their structural morphology is vastly different from those materials that are reported in this work. This molecule does not contain a tetrahedrally coordinated aluminum atom and it was synthesized upon slow hydrolysis of aluminum solution which makes the conditions irrelevant for those for the coagulation processes.[58]

With the structural characterization of the polyaluminum species, a mechanism for the formation of the Al_{32}-IDA can be inferred (Figure 3.5). The partially hydrolyzed aluminum solution, which is the primary starting material for the synthesis of Al_{32}-IDA,

contains a considerable amount of ε-Al_{13} polycation along with some monomers and dimers in solution. With the addition of the IDA, the monomeric species in solution become more reactive and complex with IDA. Upon heating and additional hydrolysis the ε-Al_{13} transforms to the δ-Al_{13} isomer which is a mandatory step in assembling these small molecular species into larger polynuclear materials. Al_{30} polycation is formed via making OH bridges with the monomers. The chelated aluminum atoms are bonded to the cluster through the deprotonation of the water molecules in the central aluminum belt, making an aluminum polycation with the Al_{32}-IDA topology. The presence of organic and inorganic anionic species such as IDA and sulfate could be important as they can prevent further hydrolysis of aluminum species and enhance coagulation of them into amorphous flocculants.

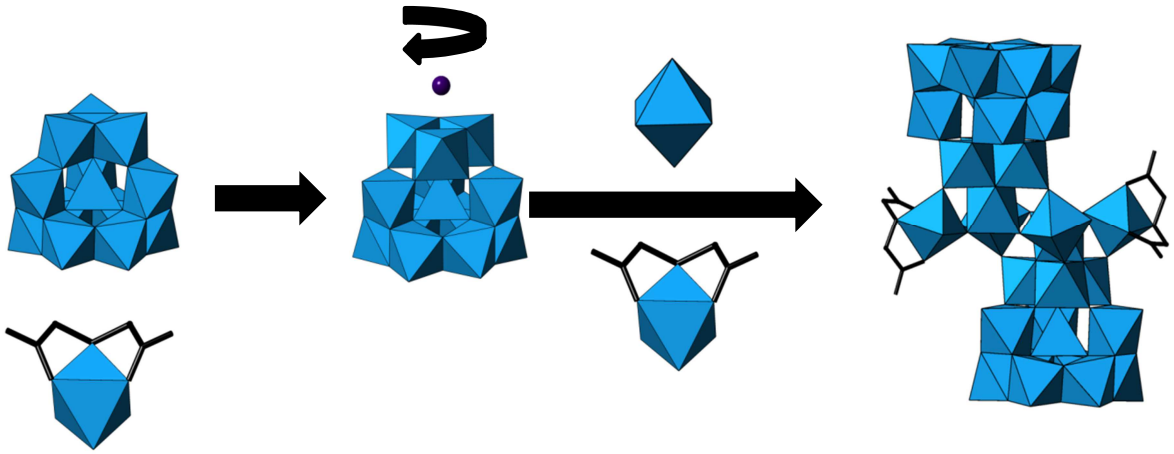

Figure 3.5 Mechanism for the formation of Al_{32}-IDA

Addition of IDA to the solution at a pH of 4.5 did not allow the IDA to bond to the surface of the ε-Al_{13} keggin but instead it is more likely to form monomeric and dimeric

species in solution. (Figure 3.5) This is quite expected as the deprotonation of the terminal water molecules of the Keggins does not take place until a pH of 5-7. Even at higher pH values the deprotonation of the IDA molecule does not cease, but instead it has to compete with the hydrolysis reactions involving aluminum in solutions. Larger polynuclear species are expected to have a less reactivity compared to the monomers due to steric constraints and therefore the organics bind to the monomers relatively easily. The chelated aluminums bind to larger polynuclear species with the deprotonation of the terminal water molecules, leading to the aggregation and the formation of flocculants with the seizing of the organic molecule.

The presence of polyaminocarboxylates in solution during hydrolysis of aluminum has been suggested to suppress the formation of the Keggin-type polycations. Interference by these compounds and other organic molecules has been suggested a potential reason as to why Keggin-type species are not more prevalent in environmental systems even though the presence of Al_{13} should be possible with total Al concentrations greater than 10-5 mol/L. The existence of epsilon-Al_{13} in the water from organic horizon of aluminum rich spodosol soils, was observed by Hunter and Ross, 1991, but undetected by Hiradate et al., 1998. Equilibrium calucations by Gerard et al., 2001 concluded that Al_{13} should be negligible in natural soils and surface waters due to the presence of interfering species. The solutions in which Al_{32}-IDA was isolated contains preformed Keggin-type moieties, thus the presence of IDA did not impact their formation.

Interestingly, IDA did not seem to significantly enhance the breakdown of the Keggin-type polycations in solution, contrary to previously reported experiments with tartaric acid, oxalate, malonate, salicylate, phthalate, and benzoate. Amirbahman et al,

2000 found that through and symbiotic chelation with carboxylatic acids and protonation of the Al_{13} solution leads to an enhanced decomposition rate. Breakdown of the Al_{13} Keggin was also noted in the presence of humic acid after precipitation into an amorphous flocculant and prolonged aging. Amirbahman et al., 2000 suggested that a bidentate coordination of the ligand to the surface of the polycation is required for the decomposition and that reactivity may be controlled by water exchange rates. As the IDA molecule chelates the aluminum atom in a tridentate fashion, it is unlikely to form a bidentate linkage to the Al_{13} molecule and there is less exchangeable water to promote the breakdown. In addition, the strong interactions between the IDA and the monomeric species suggest that the complex is stable and will not interact the polynuclear species. Monomeric species with small carboxylic acids such as oxalate or malonate have not been isolated and structural characterized, although there are some spectroscopic and computational studies that suggest their existence in solution.

The differences observed between the decomposition of the Keggin-type complexes stress the variable interactions that different organic contaminants may have with aluminum coagulants. As the chemistry associated with the various contaminants is quite unique, the one-size-fits all approach may not be able to address the suite of organic contaminants within wastewater streams. However, coagulants can potentially be optimized to target in a slightly more specific manner, to the organic contaminants of interest.

3.6.3 Optimization of PACl coagulants

Aluminum sulfate coagulants are generally ineffective at removing persistent organic contaminants from solution with less than 10% efficiency.[59] PACl-Al_{13} faired better with the removal of up to 32% of Bisphenol A from solution. The research suggests that adsorption of most organic contaminants occurs on the available organic matter in solution and not on the aluminum coagulants. Some removal then occurs with the large humic matter which is removed through sweep flocculation and the rest remains in solution.

PACl-Al_{30} may be more effective at removing contaminants as evidence by recent study by Mertens et al., 2012 that indicates an improved removal efficieicny of arsenic over broader dosage and pH range. Even though the IDA did not complex to the Keggin moieties at the pH range in this study, they were still able to be adsorbed to the surface of the Al_{30} molecule. The location of the IDA molecule on the Al_{32} polycation suggests that the central belt of octahedrally coordinated aluminum atoms is more likely to be the reactive sites where adsorption of organic molecules and other contaminants (arsenic) likely occurs. This is in agreement with molecular simulations of Al_{30} polycations performed by Rustad, 2005 [60] that suggests the H_2O groups on the central belt of octahedrally coordinated aluminum atoms more readily deprotonated than the H_2O and OH groups associated with the Keggin-like moieties. In addition, the model finds that at a pH of 5.5 these sites are more than 90% deprotonated, thus a majority of the time the Al_{30} polycation has a 16+ charge in solution.[60] In addition, the recently synthesized Al_{32}-S molecule also contains an adsorbed sulfate in a similar location as the IDA molecule, lending additional insight into contaminant adsorption by the Al_{30} molecule.

As additional deprotonation of the Al_{30} molecule will occur at increased pH, then aggregation and additional adsorption can occur, increasing sweep flocculation and enhanced removal of contaminants. The Al_{30} molecules developed the strongest floc formation and showed highest turbidity removal overall wider range of pH when compared to Al_{13} and aluminum sulfate coagulants. The isolation of the Al_{32}-IDA molecule also suggests that functionalization of the Al_{30} polycation is possible and may enhance the variety of organic functional groups that could be targeted by coagulants.

CHAPTER 4

STRUCTURE AND CHARACTERIZATION OF TRANSITION METAL CONTAINING POLYALUMINUM CLUSTERS: IMMOBILIZATION OF HEAVY METAL CATIONS IN THE ENVIRONMENT

4.1 Introduction

Having high concentrations of the metal ions in the soils can cause prolonged risks to humans and other organisms including plants. The solubility of heavy metals is quite low in the calcareous soils but the solubility increases with the neutral or acidic solutions. The remobilization of these metal cations can increase the contamination of ground water. Uptake of the metal cations by the plants can increase the concentration of those at higher levels of food chains. Traditional soil remediation methods like disposal of the contaminated materials are destructive to the environment as well as expensive.[47] The heavy metals can be immobilized by using suitable binding agents without changing the pH of the medium. Mostly they are removed by adsorption or by incorporating into solid materials.

Usually clay minerals act as possible binding agents for heavy metals due to their high specific surface area and the cation exchange capacity. The clay minerals are generally negatively charged. The adsorption ability of heavy metals by the clay minerals can be modified through the addition of aluminum.[61] Polynuclear aluminum complexes such as Al_{13} can also provide binding sites for the heavy metals.[62] With prolonged aging Al_{13} can be converted into amorphous $Al(OH)_3$.[9] Al_{13} undergoes structural rearrangements incorporating small cations into the solid material. Lothenbach et. al. in

1997 has done some qualitative adsorption studies based on polynuclear aluminum compounds and have shown that the Keggin-type aluminum materials are capable of immobilizing heavy metal cations such as Ni^{2+}, Zn^{2+}, and Cu^{2+}, but the molecular level understanding of the exact mechanism as to how it takes place is yet to be evaluated.

Adsorption of metal cations in to Keggin-type aluminum polycations was considered impossible due to the exceptionally high charge on these clusters.[47] However this study represents the synthesis of metal cation adsorbed Al_{30} and Al_{32} species, **$[(Cu(H_2O)_2(\mu_2\text{-}OH)_2)_2(Al_2(\mu_4\text{-}O)_8(Al_{28}(\mu_2\text{-}OH)_{50}(\mu_3\text{-}OH)_6(H_2O)_{26}(2,6\text{-}NDS)_9(H_2O)_{52}]$-$CuAl_{30}$** and **$[(Zn(NTA)H_2O)_2(Al(NTA)(\mu_2\text{-}OH)_2)_2(Al_{30}(\mu_2\text{-}OH)_{54}(\mu_3\text{-}OH)_6(\mu_4\text{-}O)_8(H_2O)_{20}(2,6\text{-}NDS)_5(H_2O)_{64}]$- $ZnAl_{32}$**, respectively.

4.2 Synthesis of Transition Metal Containing Keggin-type Polyaluminum Clusters

Synthesis of the aluminum clusters containing transition metal cations requires a solution which contains ε-Al_{13} nano clusters in solution. Al_{13} is thought to form in aqueous solutions during hydrolysis reactions.[63, 64] The synthesis procedure was a modified version of a method previously reported by Greg Johansson in 1960.[65] In this synthesis procedure, an aluminum chloride solution was hydrolyzed using 2.5 equivalents of sodium hydroxide without forming aluminum hydroxide precipitate. To induce crystallization a sodium selenate solution had been used which resulted in tetrahedral crystals.

4.2.1 Preparation of Al_{13} stock solution

A partially hydrolyzed aluminum stock solution was prepared by heating 25 mL of 0.25 M $AlCl_3$ (6.25 mmol) solution to 80 ^{0}C in a water bath. This was followed by drop wise addition of 60 mL of 0.25 M NaOH (6.25 mmol) to a hydrolysis ratio (OH^-/Al^{3+}) of 2.4.

4.2.2 Synthesis of $CuAl_{30}$ cluster $[(Cu(H_2O)_2(\mu_2\text{-}OH)_2)_2(Al_2(\mu_4\text{-}O)_8(Al_{28}(\mu_2\text{-}OH)_{50}(\mu_3\text{-}OH)_6(H_2O)_{26}(2,6\text{-}NDS)_9(H_2O)_{52}]$

Approximately 7 mL of the cooled Al_{13} stock solution was mixed with 0.0349 g of Trizma base and 0.0382 g of $CuCl_2$. The dark blue color mixture was stirred for 20 min and loaded in to a Teflon-lined Parr reaction vessel and heated to 80 ^{0}C in a gravimetric oven for 24 hours. The resultant solution was transferred to a 23 mL scintillation vial along with 3 mL of 0.1 M 2, 6-NDS. The contents were mixed well and allowed for slow evaporation in the fume hood. After about 14 days, light-blue transparent blade-like crystals were formed which were suitable for single crystal X-ray diffraction studies.

4.2.3 Synthesis of $ZnAl_{32}$-NTA cluster $[(Zn(NTA)H_2O)_2(Al(NTA)(\mu_2\text{-}OH)_2)_2(Al_{30}(\mu_2\text{-}OH)_{54}(\mu_3\text{-}OH)_6(\mu_4\text{-}O)_8(H_2O)_{20}(2,6\text{-}NDS)_5(H_2O)_{64}]$

Approximately 7 mL of the cooled Al_{13} stock solution was mixed with 0.0308 g of $ZnCl_2$ and 0.0345 g of Nitrilotriacetic acid (NTA). The mixture was stirred for 20 min and loaded in to a Teflon-lined Parr reaction vessel and heated to 80 ^{0}C in a gravimetric oven for 24 hrs. Afterwards the mixture was cooled and transferred to a 23 mL scintillation vial along with 3 mL of 0.1 M 2, 6 NDS. The contents were mixed well and

allowed for slow evaporation in the hood. After about 21 days colorless blocky crystals were formed that were suitable for single crystal X-ray diffraction studies.

4.2.4 Structural Characterization of the compounds

Data collection, refinement and structure solution of the clusters were done according to the method explained in section 2.3. $CuAl_{30}$ crystallized in the triclinic space group *P*-1 with a = 18.323(5), b = 18.469(5), c =24.985(8), α = 73.966(10), β = 80.078(10), and γ =62.392(9). $ZnAl_{32}$-NTA also crystalizes in *P-1* with unit cell parameter refined as a = 16.733(7) (5), b = 18.0.34(10), c =21.925(11), α = 82.821(19) (10), β = 70.958(17), and 65.362(18). Selected data collection parameters are given in table 4.1 and selected bond distance for $CuAl_{30}$ and $ZnAl_{32}$-NTA are given in Tables 4.2 and 4.3.

Structural disorder is prominent in the naphthalene rings, solvent waters and the oxygen atoms from the disulfonate moieties. Disorder associated with the sulfonate groups is mainly due to the free rotation about the S-C bond and this leads to the elongation of the electron density around oxygen atoms. Due to this reason about four oxygen atoms were modeled as split sites and they were O52 (A, B), O53 (A, B), O55 (A, B), and O74 (A, B) each with 50% occupancy. Disorder was associated with one of the naphthalene rings in particular and it was modeled using the DFIX command. The diffuse electron density of the water molecules was modeled using the SQUEEZE command in the PLATON software[38] which enabled to reduce the R_1 value from 11.89% to 8.8%.

Table 4.1 Selected Crystallographic information for $CuAl_{30}$ and $ZnAl_{32}$-NTA

	$CuAl_{30}$	$ZnAl_{32}$-NTA
a(Å)	18.323(5)	16.733(7)
b (Å)	18.469(5)	18.0.34(10)
c (Å)	24.985(8)	21.925(11)
α (°)	73.966(10)	82.821(19)
β (°)	80.078(10)	70.958(17)
γ (°)	62.392(9)	65.362(18)
V ($Å^3$)	7191(4)	5672(5)
Z	1	1
FW($gmol^-$)	6218.5	6109.2
Space Group	*P*-1	*P-1*
ρ_{calc} (g/cm^3)	1.291	1.568
μ (mm^{-1})	0.471	0.556
F(000)	2798	2682
Crystal Size (mm)	0.192 x 0.18 x 0.095	0.138 x 0.128 x 0.98
Theta range	1.48 to 25.06°	0.98 to 26.07°
Data collected	-21<h<21, -21<k<21, -29<l<29	-20<h<20, -22<k<21, -27<l<27
Completeness to theta = 26.07°	99.2%	98.0%
Reflections collected/unique	135761 / 25292	81079 / 22005
GOF on F^2	1.082	1.067

Table 4.1 continued.

Final R indices [I> 2σ(I)]	$R_1 = 0.0818, wR_2 = 0.2456$	$R_1 = 0.0913, wR_2 = 0.2774$
R indices (all data)	$R_1 = 0.1025, wR_2 = 0.2634$	$R_1 = 0.1042, wR_2 = 0.2906$
Largest diff. peak and hole (Å^3)	2.141 and -1.077	4.361 and -3.191

4.3 Structural Description

4.3.1 Structural description of the basic aluminum polynuclear species (Al_{30})

Both molecular species contained an Al_{30} clusters, which is built upon the Keggin-type δ-Al_{13} moiety. The δ-Al_{13} cluster consists of a central Al^{3+} cation tetrahedrally coordinated to four oxygen atoms. The bond lengths vary from 1.795(7) – 1.830(6) Å. The $Al(O)_4$ tetrahedron is surrounded by twelve octahedrally coordinated Al^{3+} cations with bond lengths varying from 1.839(6) – 2.06(6) Å. The octahedral aluminum groups are arranged in to four planar $[Al_3(\mu_2\text{-}OH)_6(H_2O)_3]$ trimers through edge sharing of hydroxyl groups. (Figure 4.1) With further corner and edge sharing, these trimers surround the central $Al(O)_4$ unit to form a tridecamer, $[Al(\mu_4\text{-}O_4)Al_{12}(\mu_2\text{-}OH)_{24}(H_2O)_{12}]^{7+}$ with an approximate diameter of one nanometer.

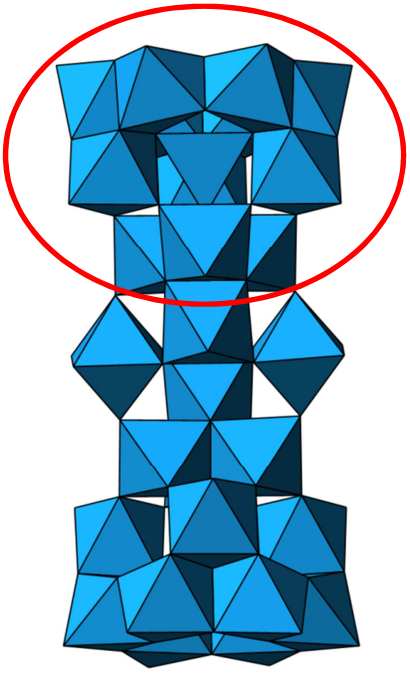

Figure 4.1 Al_{30} polycation with the δ- Al_{13} - the basic building block circled in red

The Al_{30} polycation is formed via the combination of two δ- Al_{13} units through four additional octahedrally coordinated Al^{3+} cations. (Figure 4.1) These clusters are about 2 nm in diameter and were previously isolated by using sulfate and 2, 6-naphthalene disulfonate.[20, 22, 23]

4.3.2 Structure of $CuAl_{30}$

The $CuAl_{30}$ compound contains the large Al_{30} polynuclear species with Cu^{2+} bonded to the exterior of the cluster. (Figure 4.2) There are two Cu^{2+} cations per Al_{30} molecule and they are coordinated to two aluminum atoms through Al-O bonds and to two water molecules forming a square planar environment around copper. The Al-O bond length varies from 1.921(3) – 2.007(4) Å. Cu-O bonds have varying bond lengths in the range of 1.921-2.007 Å. In addition, there are two other oxygen atoms, one from a

solvent water molecule and the other from a sulfonate group of a 2, 6-NDS molecule, placed at distances of 2.572 Å and 2.589 Å from Cu^{2+} respectively.

Cu^{2+} can form hexa-coordinated compounds quite frequently and in some of these compounds tetragonal or Jahn Teller Distortion is commonly observed owing to the d^9 electron configuration of copper. The latter two bonds can be considered as long Cu-O axial bonds showing (4+2) coordination due to the Jahn-Teller effect. Table 4.4 shows a list of chemical compounds that possess long Cu-O bonds. Compound 1 in particular shows long Cu-O axial bonds with 2.482 Å and these oxygen atoms belong to sulfate groups which is in resemblance to one of the Cu-O bonds in our compound. In addition there are other copper compounds in literature with bond lengths ranging from 2.5-2.7 Å which clearly suggests the presence of Jahn Teller distortion.

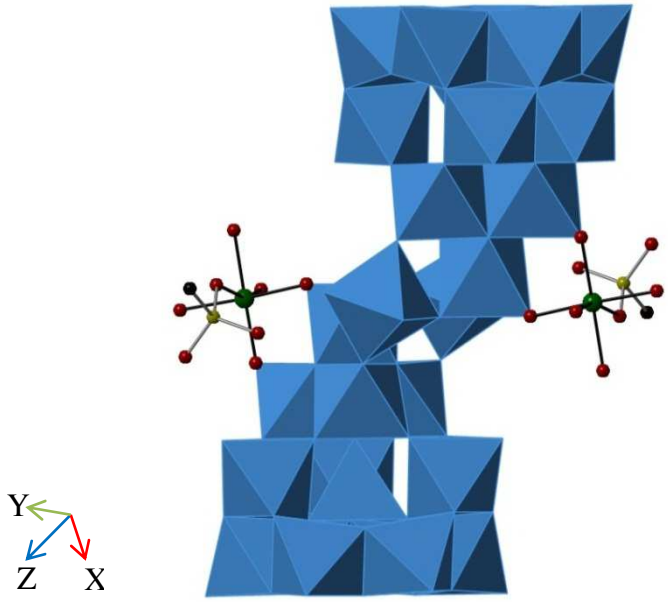

Figure 4.2 A polyhedral representation of Al_{30} polycation with Cu^{2+} adsorption (Cu-green, Al-blue, O-red, S-yellow, C-black)

Table 4.2 Selected bond lengths (Å) and angles (degrees) of $CuAl_{30}$

Cu(1)-O(26)	1.921(3)	Al(12)-O(60)	1.775(3)
Cu(1)-O(5)	1.948(3)	Al(12)-O(15)	1.782(3)
Cu(1)-O(49)	1.969(4)	Al(12)-O(30)	1.795(3)
Cu(1)-O(50)	2.007(4)	Al(12)-O(23)	1.837(3)
Al(1)-O(12)	1.830(3)	Al(13)-O(25)	1.844(4)
Al(1)-O(2)	1.833(3)	Al(13)-O(17)	1.852(4)
Al(1)-O(8)	1.858(3)	Al(13)-O(18)	1.852(4)
Al(1)-O(45)	1.955(3)	Al(13)-O(14)	1.884(4)
Al(1)-O(27)	1.957(3)	Al(13)-O(46)	1.944(4)
Al(1)-O(23)	1.964(3)	Al(13)-O(30)	2.015(3)
Al(2)-O(5)	1.811(3)	Al(14)-O(20)	1.829(4)
Al(2)-O(11)	1.861(3)	Al(14)-O(4)	1.847(4)
Al(2)-O(9)	1.868(3)	Al(14)-O(33)	1.852(3)
Al(2)-O(27)	1.921(3)	Al(14)-O(32)	1.857(4)
Al(2)-O(45)	1.950(3)	Al(14)-O(29)	1.935(4)
Al(2)-O(28)	1.959(3)	Al(14)-O(15)	2.073(3)
Al(3)-O(8)	1.872(3)	Al(15)-O(4)	1.832(4)
Al(3)-O(11)[a]	1.884(3)	Al(15)-O(25)	1.855(4)
Al(3)-O(9)	1.886(3)	Al(15)-O(34)	1.877(4)

Table 4.2 continued.

Al(3)-O(21)	1.890(3)	Al(15)-O(14)	1.878(4)
Al(3)-O(24)	1.946(3)	Al(15)-O(48)	1.939(4)
Al(3)-O(35)	1.975(3)	Al(15)-O(15)	1.986(3)
Al(4)-O(19)	1.834(3)	S(1)-O(65)	1.425(5)
Al(4)-O(26)	1.841(3)	S(1)-O(61)	1.434(4)
Al(4)-O(7)	1.844(3)	S(1)-O(62)	1.447(4)
Al(4)-O(28)	1.941(3)	S(1)-C(28)	1.765(5)
Al(4)-O(27)	1.950(3)		
Al(4)-O(23)	2.004(3)	S(2)-O(40)	1.436(4)
		S(2)-O(39)	1.442(4)
Al(5)-O(36)	1.847(3)	S(2)-O(41)	1.460(4)
Al(5)-O(37)	1.859(4)	S(2)-C(29)	1.772(5)
Al(5)-O(10)	1.864(3)		
Al(5)-O(3)	1.871(3)	S(3)-O(52A)	1.364(8)
Al(5)-O(47)	1.939(4)	S(3)-O(53B)	1.391(8)
Al(5)-O(60)	2.007(3)	S(3)-O(51)	1.425(4)
		S(3)-O(53A)	1.550(9)
Al(6)-O(1)	1.856(3)	S(3)-O(52B)	1.575(9)
Al(6)-O(31)	1.877(3)	S(3)-C(32)	1.767(5)
Al(6)-O(2)	1.879(3)		
Al(6)-O(3)	1.886(3)	S(4)-O(63)	1.416(4)

Table 4.2 continued.

Al(6)-O(6)	1.938(4)	S(4)-O(64)	1.422(5)
Al(6)-O(60)	1.949(3)	S(4)-O(66)	1.472(6)
		S(4)-C(35)	1.777(6)
Al(7)-O(16)	1.863(3)		
Al(7)-O(34)	1.875(4)	S(5)-O(42)	1.422(4)
Al(7)-O(33)	1.888(3)	S(5)-O(43)	1.422(5)
Al(7)-O(19)	1.899(3)	S(5)-O(44)	1.451(6)
Al(7)-O(13)	1.929(4)	S(5)-C(31)	1.760(6)
Al(7)-O(15)	1.949(3)		
		S(6)-O(58)	1.363(7)
Al(8)-O(7)	1.874(3)	S(6)-O(57)	1.412(5)
Al(8)-O(17)	1.881(4)	S(6)-O(59)	1.508(5)
Al(8)-O(12)	1.882(3)	S(6)-C(38)	1.757(7)
Al(8)-O(22)	1.890(3)		
Al(8)-O(38)	1.927(4)	S(7)-O(54)	1.458(6)
Al(8)-O(30)	1.949(3)	S(7)-O(56)	1.472(6)
		S(7)-O(55B)	1.473(9)
Al(9)-O(18)	1.851(4)	S(7)-O(55A)	1.509(9)
Al(9)-O(37)	1.861(3)	S(7)-C(37)	1.767(7)
Al(9)-O(10)	1.862(4)		
Al(9)-O(22)	1.870(3)	S(8)-O(73)	1.434(5)
Al(9)-O(67)	1.929(4)	S(8)-O(71)	1.438(6)

Table 4.2 continued.

Al(9)-O(30)	2.042(3)	S(8)-O(72)	1.463(7)
		S(8)-C(42)	1.700(8)
Al(10)-O(36)	1.827(4)		
Al(10)-O(20)	1.838(4)	S(9)-O(75)	1.290(14)
Al(10)-O(31)	1.859(3)	S(9)-O(74B)	1.454(12)
Al(10)-O(32)	1.860(4)	S(9)-O(74A)	1.670(2)
Al(10)-O(68)	1.946(4)	S(9)-C(45)	1.837(13)
Al(10)-O(60)	2.062(3)		
		O(26)-Cu(1)-O(5)	93.42(13)
Al(11)-O(16)	1.828(3)	O(26)-Cu(1)-O(49)	89.43(16)
Al(11)-O(1)	1.833(3)	O(5)-Cu(1)-O(49)	174.40(15)
Al(11)-O(21)[a]	1.862(3)	O(26)-Cu(1)-O(50)	174.04(17)
Al(11)-O(28)	1.949(3)	O(5)-Cu(1)-O(50)	87.54(15)
Al(11)-O(45)	1.954(3)	O(49)-Cu(1)-O(50)	90.11(17)
Al(11)-O(23)	2.002(3)		

Symmetry transformations used to generate equivalent atoms; a) -x+1,-y+1,-z+1

In addition, bond valence calculations were also done for this cluster in order to verify the coordination environment around Cu. Copper in its square planar environment provides a bond valence of 1.5961 vu whereas for the octahedral geometry it's about 1.6690 vu. The calculations were done using a B value of 0.37 Å which is derived for a perfect octahedron and as the B value is influenced by distortion of the octahedron (as

seen for the uranyl polyhedra) that may result in a low valence unit for Cu^{2+}. Details of the bond valence calculations are included in the Appendix.

Table 4.3 Evidence from literature for Jahn-Teller effect

	Compound	Cu-O Bond length (Å)	
		axial	equatorial
1	$(C_7H_{10}N)_2[Cu(SO_4)_2(H_2O)_4]$[66]	2.482	1.947-1.9710
2	$Cu_3C_{36}H_{40}N_6O_{20}S_2$[67]	2.523- 2.605	1.923–2.005
3	$[Cu(C_7H_2O_6)(H_2O)_4]$[68]	2.447-2.525	1.906-1.982
4	$[Cu(enMe)_2]_3[As_3Mo_3O_{15}]_2.2H_2O$[69]	2.543-2.635	
5	$[pipH_2][Cu(ox)_2(H_2O)_2] \cdot 2H_2O$[70]	2.540	1.935-1.962
6	$\{(4\text{-}pyOH_2)_2[Cu(CA)_2(H_2O)_2]\}_n$[71]	2.623	1.962-1.937
7	$(C_5H_7N_2)_2[Cu(C_3H_2O_4)_2(H_2O)_2]$[72]	2.665	1.9293-1.9336
8	$[Cu(C_6H_5O_5)_2(H_2O)_2]$[73]	2.515	
9	$[\{Cu(en)_2\}_4Cu(H_2O)_2H_2W_{12}O_{42}]H_2O$ [74]	2.550-2.631	1.950-1.965
10	$\{[Cu_2(ptec)(py)_2(H_2O)_3].\ 4H_2O\}_n$[75]	2.533	1.972-1.950
11	$[M(H_2O)_6][Cu(mal)_2(H_2O)_2]$ (M=Mn, Co, Ni, Cu, Zn)[76]	2.445-2.480	1.942-1.950

These aluminum polycations form a three dimensional molecular network with the aid of hydrogen bonding formed between the cluster and the deprotonated disulfonate anions. There are nine 2, 6-NDS anions per unit cell leading to the overall formula $[(Cu(H_2O)_2(\mu_2\text{-}OH)_2)_2(Al_2(\mu_4\text{-}O)_8(Al_{28}(\mu_2\text{-}OH)_{50}(\mu_3\text{-}OH)_6(H_2O)_{26}](2,6\text{-}NDS)_9$. Additional hydrogen bonding is present in the structure between the deprotonated oxygen on disulfonate anions and the hydrogen atoms of the OH and H_2O molecules of the aluminum polycations. The disulfonates are arranged in different orientations within the void spaces of these structures which are facilitated by the occurrence of hydrogen bonding, steric effects and π-π interactions of the naphthalene rings. Solvent water molecules are also present in the void spaces of these structures forming hydrogen bonds with the aluminum polycations and the disufonates resulting in a three-dimensional crystal lattice.

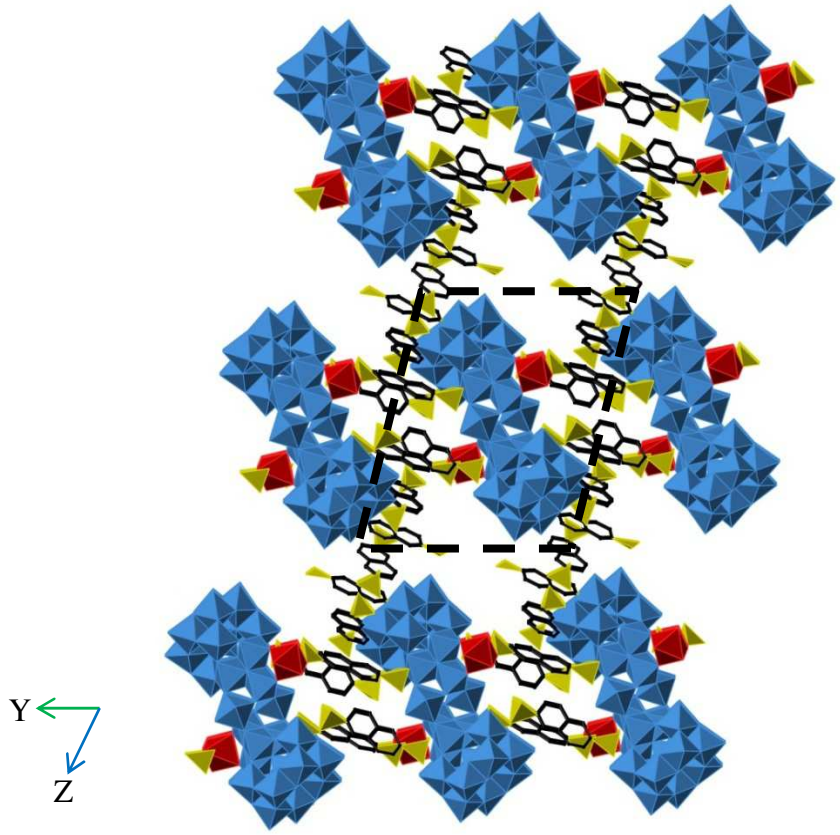

Figure 4.3 Three dimensional molecular network formed by $CuAl_{30}$

4.3.3 Structure of $ZnAl_{32}$-NTA

The $ZnAl_{32}$-NTA compound contains Al_{30} polycation with two additional Al and Zn cations complexed by Nitrilotriacetic acid (NTA) which is coordinated to the exterior of the cluster. The aluminum atoms are joined to Keggin-type cluster in a bridging-bidentate fashion. These two aluminum atoms are also coordinated to two NTA molecules in a tetradentate manner via three oxygen atoms and a nitrogen atom in the NTA molecule completing the octahedral environment. The Al-O and Al-N bond distances are from 1.865(4) – 1.913(4) Å and 2.114(5) Å, respectively. In addition Zn^{2+} cation is coordinated to one of the aluminum atoms that acts as the linker between the two δ-Al_{13} moieties, through an oxygen atom with a bond length of 1.879(4) Å. The zinc atom is bonded tetrahedrally to a NTA molecule and a water molecule is also there to complete the octahedral coordination environment around it. The Zn-O bond distance varies from 1.879(4) – 2.056(6) Å whereas the Zn-N bond distance is around 2.153(5) Å.

The $ZnAl_{32}$-NTA forms a three dimensional molecular network structure with the aid of hydrogen bonding that occurs with the deprotonated disulfonate molecules. There are five disulfonate molecules per unit cell and the deprotonated sulfonate molecules form hydrogen bonding with the hydrogen atoms of OH groups and H_2O molecules in the aluminum polycation. In addition to the hydrogen bonding, these compounds are expected to have weak Van der Waals and π-π interactions with the naphthalene rings of the 2,6 NDS. It can be inferred that the crystallization from an aqueous solution is facilitated by the 2,6 NDS due to their larger size, negative charge, and the potential Van der Waals, hydrogen and π-π interactions.

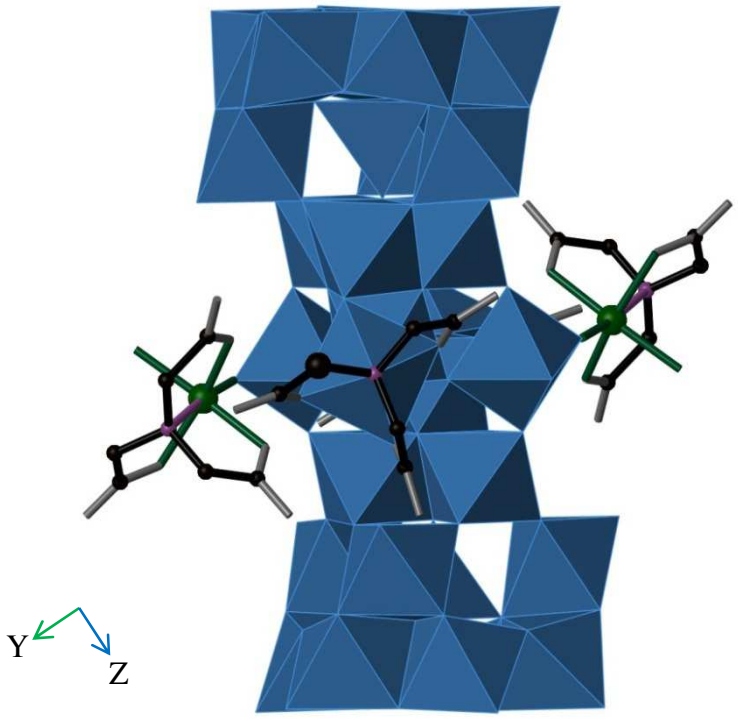

Figure 4.4 A Polyhedral representation of $ZnAl_{32}$-NTA aluminum polycation (Zn- green, Al- blue, N- purple, O- grey, C- black)

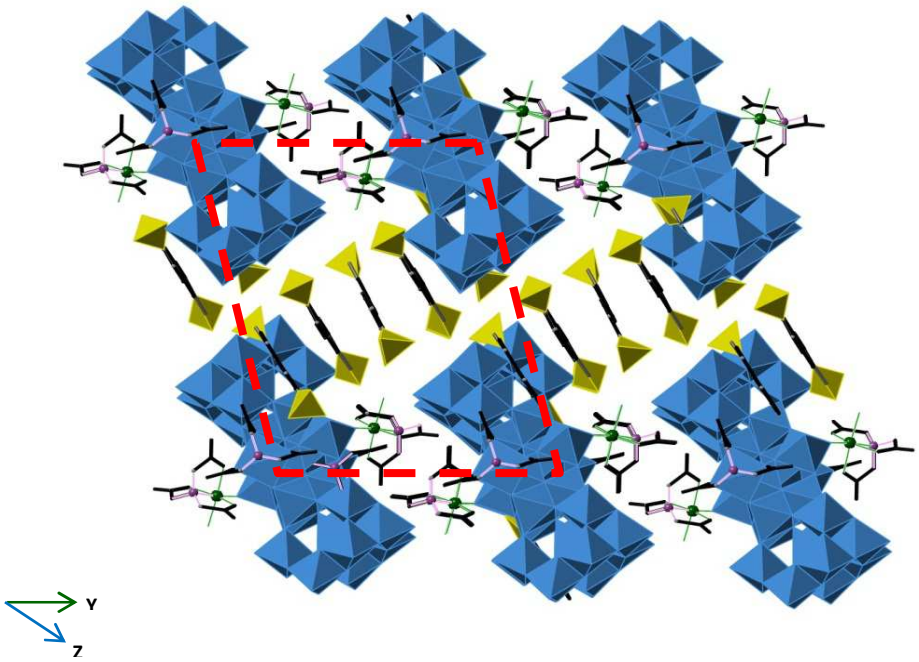

Figure 4.5 Three dimensional molecular network structure formed by $ZnAl_{32}$-NTA (Al- blue, Zn- green, N- purple, O- grey, C- black, S- yellow)

Table 4.4 Selected bond lengths (Å) and angles (degrees) of $ZnAl_{32}$-NTA

Zn(1)-O(32)	1.879(4)	Al(11)-O(13)	1.860(4)
Zn(1)-O(31)	1.996(4)	Al(11)-O(20)	1.939(4)
Zn(1)-O(56)	2.016(4)	Al(11)-O(1)	2.070(4)
Zn(1)-O(55)	2.048(4)		
Zn(1)-O(68)	2.056(6)	Al(12)-O(9)	1.850(4)
Zn(1)-N(1)	2.153(5)	Al(12)-O(33)	1.854(4)
		Al(12)-O(23)	1.871(4)
Al(1)-O(10)	1.865(4)	Al(12)-O(34)	1.875(4)
Al(1)-O(17)	1.882(4)	Al(12)-O(53)	1.934(4)
Al(1)-O(41)	1.905(4)	Al(12)-O(11)	2.042(4)
Al(1)-O(42)	1.907(4)		
Al(1)-O(24)	1.913(4)	Al(13)-O(6)	1.841(4)
Al(1)-N(2)	2.114(5)	Al(13)-O(40)	1.858(4)
		Al(13)-O(50)	1.869(4)
Al(2)-O(3)	1.830(4)	Al(13)-O(46)	1.888(4)
Al(2)-O(39)	1.845(4)	Al(13)-O(36)	1.943(4)
Al(2)-O(7)	1.853(4)	Al(13)-O(1)	2.030(4)
Al(2)-O(35)	1.965(4)		
Al(2)-O(12)	1.966(4)	Al(14)-O(44)	1.865(4)
Al(2)-O(29)	1.988(4)	Al(14)-O(5)	1.889(4)
		Al(14)-O(46)	1.901(4)
Al(3)-O(23)	1.866(4)	Al(14)-O(4)	1.910(4)

Table 4.4 continued.

Al(3)-O(2)	1.876(4)	Al(14)-O(26)	1.924(4)
Al(3)-O(3)	1.886(4)	Al(14)-O(1)	1.940(4)
Al(3)-O(22)	1.898(4)		
Al(3)-O(30)	1.917(4)	Al(15)-O(16)	1.846(4)
Al(3)-O(11)	1.971(4)	Al(15)-O(33)	1.854(4)
		Al(15)-O(34)	1.859(4)
Al(4)-O(2)	1.829(4)	Al(15)-O(25)	1.878(4)
Al(4)-O(5)	1.839(4)	Al(15)-O(65)	1.935(5)
Al(4)-O(37)	1.878(4)	Al(15)-O(15)	2.047(4)
Al(4)-O(29)	1.944(4)		
Al(4)-O(38)	1.949(4)	Al(16)-O(1)	1.787(4)
Al(4)-O(12)	2.026(4)	Al(16)-O(11)	1.794(4)
		Al(16)-O(15)	1.805(4)
Al(5)-O(37)	1.892(4)	Al(16)-O(12)	1.834(4)
Al(5)-O(39)[a]	1.898(4)		
Al(5)-O(32)	1.900(4)	S(1)-O(45)	1.442(4)
Al(5)-O(28)[a]	1.909(4)	S(1)-O(49)	1.461(5)
Al(5)-O(14)	1.927(4)	S(1)-O(57)	1.475(5)
Al(5)-O(43)	1.966(4)	S(1)-C(5)	1.777(6)
Al(6)-O(4)	1.840(4)	S(2)-O(64)	1.444(7)
Al(6)-O(8)	1.864(4)	S(2)-O(59)	1.452(7)

Table 4.4 continued.

Al(6)-O(41)	1.907(4)	S(2)-O(66)	1.460(5)
Al(6)-O(35)	1.955(4)	S(2)-C(18)	1.768(7)
Al(6)-O(38)	1.972(4)		
Al(6)-O(12)	2.015(4)	S(3)-O(61)	1.425(6)
		S(3)-O(47)	1.449(4)
Al(7)-O(25)	1.894(4)	S(3)-O(60)	1.507(7)
Al(7)-O(18)	1.897(4)	S(3)-C(17)	1.769(6)
Al(7)-O(7)	1.900(4)		
Al(7)-O(8)	1.902(4)	S(4)-O(72)	1.429(8)
Al(7)-O(19)	1.927(4)	S(4)-O(62)	1.452(7)
Al(7)-O(15)	1.940(4)	S(4)-O(58)	1.456(6)
		S(4)-C(33)	1.776(10)
Al(8)-O(10)	1.850(4)		
Al(8)-O(28)	1.858(4)	S(5)-O(67)	1.422(7)
Al(8)-O(14)	1.859(4)	S(5)-O(63)	1.437(6)
Al(8)-O(29)	1.919(4)	S(5)-O(71)	1.487(9)
Al(8)-O(38)	1.959(4)	S(5)-C(9)	1.773(6)
Al(8)-O(35)	1.975(4)		
		N(1)-C(2)	1.474(7)
Al(9)-O(13)	1.849(4)	N(1)-C(11)	1.476(7)
Al(9)-O(16)	1.856(4)	N(1)-C(12)	1.491(7)
Al(9)-O(27)	1.856(4)		

Table 4.4 continued.

Al(9)-O(18)	1.868(4)	N(2)-C(6)	1.483(7)
Al(9)-O(21)	1.931(4)	N(2)-C(10)	1.486(7)
Al(9)-O(15)	2.064(4)	N(2)-C(1)	1.488(7)
Al(10)-O(50)	1.853(4)	O(32)-Zn(1)-O(31)	104.91(16)
Al(10)-O(9)	1.855(4)	O(32)-Zn(1)-N(1)	173.48(17)
Al(10)-O(22)	1.867(4)	O(45)-S(1)-O(49)	113.4(3)
Al(10)-O(40)	1.880(4)	C(2)-N(1)-Zn(1)	107.2(3)
Al(10)-O(48)	1.965(4)		
Al(10)-O(11)	2.019(4)		
Al(11)-O(44)	1.846(4)		
Al(11)-O(6)	1.854(4)		
Al(11)-O(27)	1.857(4)		

Symmetry transformations used to generate equivalent atoms; a) -x+2,-y+2,-z b)-x+2,-y+3,-z+1

4.4 Thermogravimetric Analysis

The Thermogravimetric analysis was done on these compounds to estimate the number of water molecules in the interstitial sites. We used the SQUEEZE program in PLATON software to model the disorders of the solvents, thus we are not able to determine the actual number water molecules that should be present in the structure by

single-crystal X-ray diffraction alone. TGA was done on the ground crystalline materials as explained in section 2.6.

The interstitial water molecules are the less tightly bound solvent species found in the structure that are hydrogen bonding. During the heating process of $CuAl_{30,}$ these waters are removed from the cluster around 80-120 ^{0}C. The weight loss corresponding to the interstitial waters is about 15.14% and it accounts for 52 molecules of water. The structural water molecules associated with the polynuclear species are removed between 120 ^{0}C and 300 ^{0}C. At temperatures above 400 ^{0}C the 2,6 NDS anions decompose, liberating CO_2, H_2O and SO_x gaseous products. The organic ligands in $ZnAl_{32}$-NTA, decompose to CO_2 and H_2O around 300-400 ^{0}C. The percentage weight losses associated with the decomposition of $CuAl_{30}$ and $ZnAl_{32}$-NTA clusters are given in Table 4.5.

The theoretical percentages were calculated from the formula of the compound after accounting for the interstitial waters. The experimental weight losses were calculated based on the derivative weights found during the analysis. According to the data shown above, the experimental weight loss is a bit higher than the theoretical in almost all the occasions, which is acceptable as the decomposition of these compounds occur within a certain temperature range rather than a single temperature. The TGA graphs are shown in Figure 4.6 and 4.7 for $CuAl_{30}$ and $ZnAl_{32}$-NTA, respectively.

Table 4.5 Theoretical and Calculated weight losses associated with $CuAl_{30}$ and $ZnAl_{32}$-NTA

	$CuAl_{30}$ Weight loss (%)		$ZnAl_{32}$-NTA Weight loss (%)	
	Theoretical	Experimental	Theoretical	Experimental
Structural water	8.68	10.98	6.48	7.74
Adsorbed organics	-	-	12.32	15.00
2,6 NDS	38.0	37.0	19.83	22.48
Final product	42.74	41.24	36.3	35.81

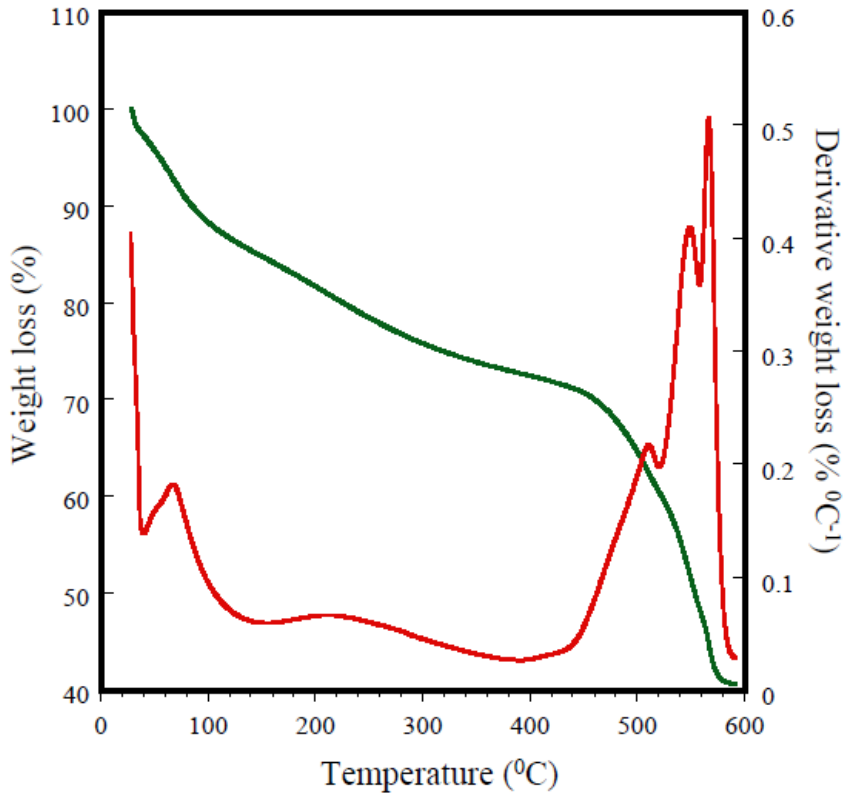

Figure 4.6 Plot for the Thermogravimetric analysis of $CuAl_{30}$

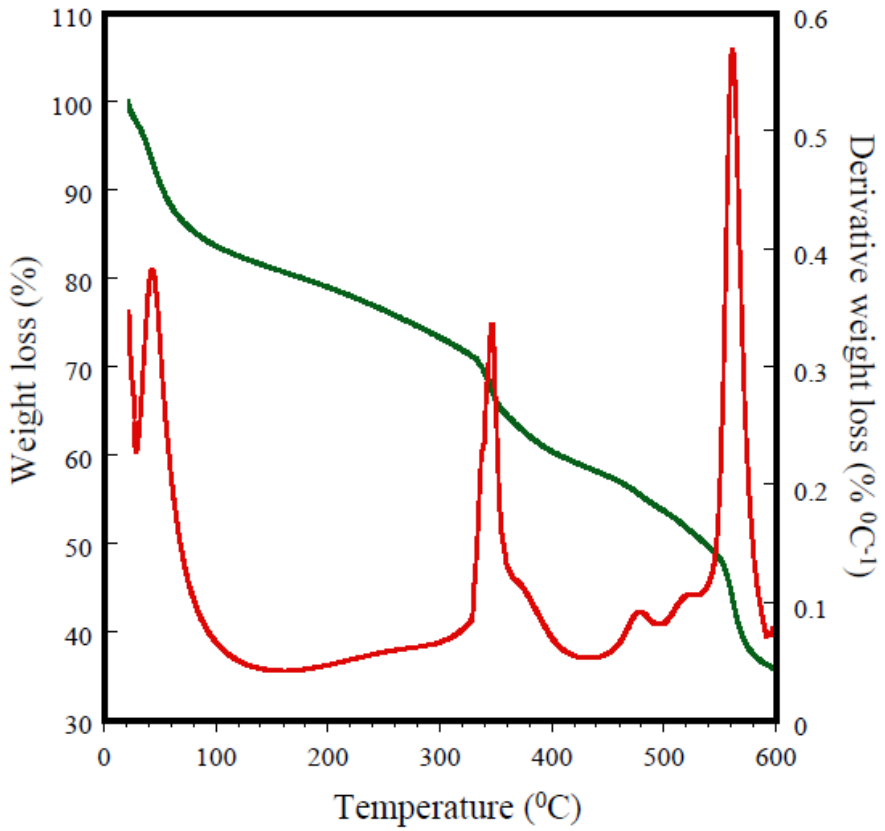

Figure 4.7 Plot for the Thermogravimetric analysis of $ZnAl_{32}$-NTA

The $CuAl_{30}$ cluster contained only a Cu^{2+} adsorbed on to the cluster with a distorted octahedral geometry through an Al-O bond. Thus the TGA did not show any significant decomposition in the range of 300-400 ^{0}C. Theoretical and experimental final weight losses were largely consistent, being 42.74 and 41.24 % respectively. This weight loss suggests the presence of 2 moles of Cu^{2+}, 30 moles of $Al(OH)_3$ and 2 moles of SO_4^{2-} per mole of $CuAl_{30}$ in the final product. Therefore we can assume that residual material is an amorphous aluminum species which is doped with Cu, which contains SO_4^{2-} that contributes in charge balancing of the compound with an empirical formula, **$[Cu_{0.07}Al(OH)_3(SO_4)_{0.07}]$.**

The TGA plot shown in Figure 4.9 for $ZnAl_{32}$-NTA appears slightly different than that of $CuAl_{30}$. There were 64 interstitial water molecules per molecule of cluster according to the TGA data. Also this cluster contains 4 molecules of NTA adsorbed on to a molecule of the cluster. NTA molecules decompose around 300-400 ^{0}C liberating CO_2 and H_2O. The decomposition of 2,6-NDS occurs at higher temperatures but the final weight percentage suggests the presence of 2 moles of Zn^{2+}, 2 moles of SO_4^{2-} and 32 moles of boehmite (γ-AlOOH) per mole of the material. So the residual compound may have an empirical formula of **[$Zn_{0.07}$(AlOOH)(SO_4)$_{0.07}$]**, which is possibly a zinc doped precursor to boehmite.

4.5 Scanning Electron Microscopy with Energy Dispersive Spectroscopy

Scanning Electron Microscopy study followed by an Energy Dispersive Spectroscopy analysis for the single crystals was done as described in section 2.5 which enabled the determination of the elemental composition of these compounds. Figure 4.8 shows the SEM image of the $CuAl_{30}$ cluster. The image depicts that the crystals have a shape of rods under a magnification of 1300x.

The EDS spectrum obtained for this compound is shown in Figure 4.9. According to the data it further suggests the presence of Cu in the synthesized crystals.

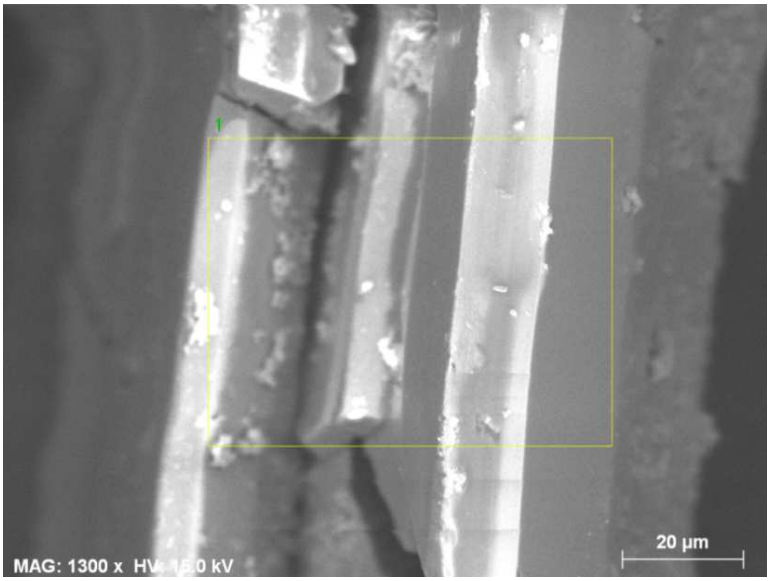

Figure 4.8 SEM image of $CuAl_{30}$ crystals

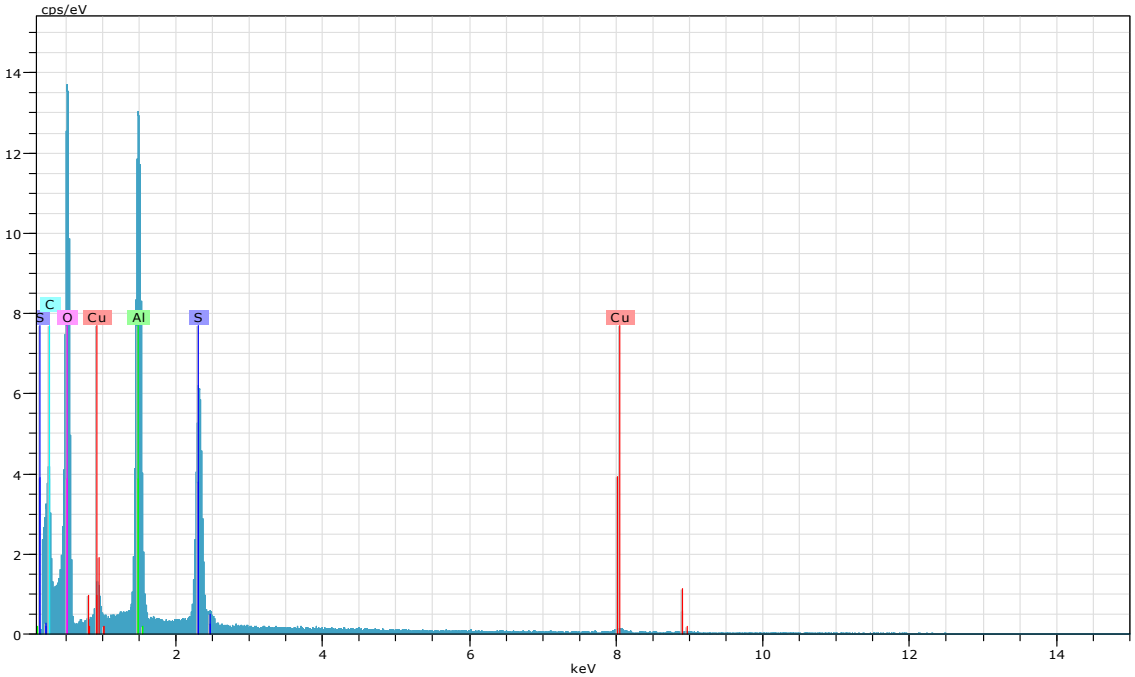

Figure 4.9 EDS spectrum of $CuAl_{30}$ crystal

In a similar manner the EDS analysis was carried out for the $ZnAl_{32}$ cluster. Figure 4.10 shows the surface image of the $ZnAl_{32}$ with a trace amount of salt impurities under a magnification of 1800x. The EDS data again suggest the presence of Zn in these compounds. (Figure 4.11)

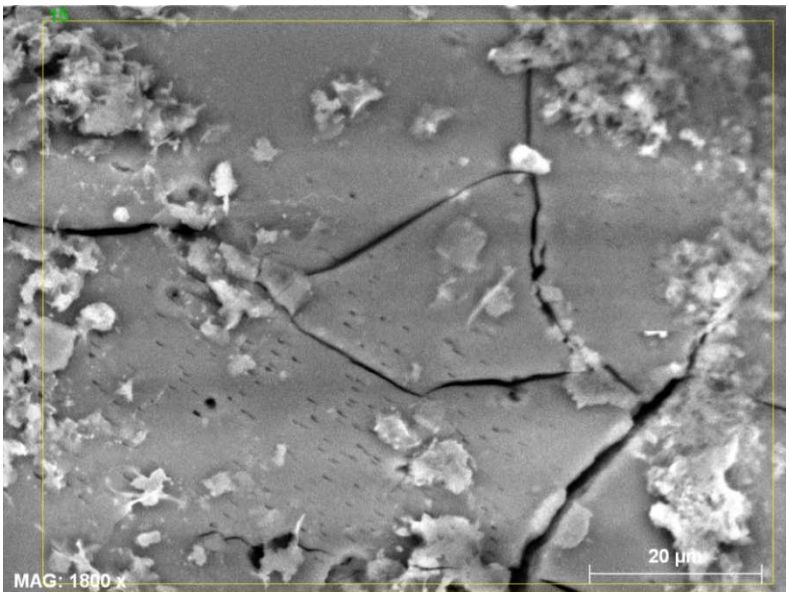

Figure 4.10 SEM image of $ZnAl_{32}$-NTA crystals

Something commonly observed in these two clusters is the rapid dehydration of the surface upon exposure to air. Clusters may lose less tightly bound water molecules contracting the crystals and rupturing the crystal surface.

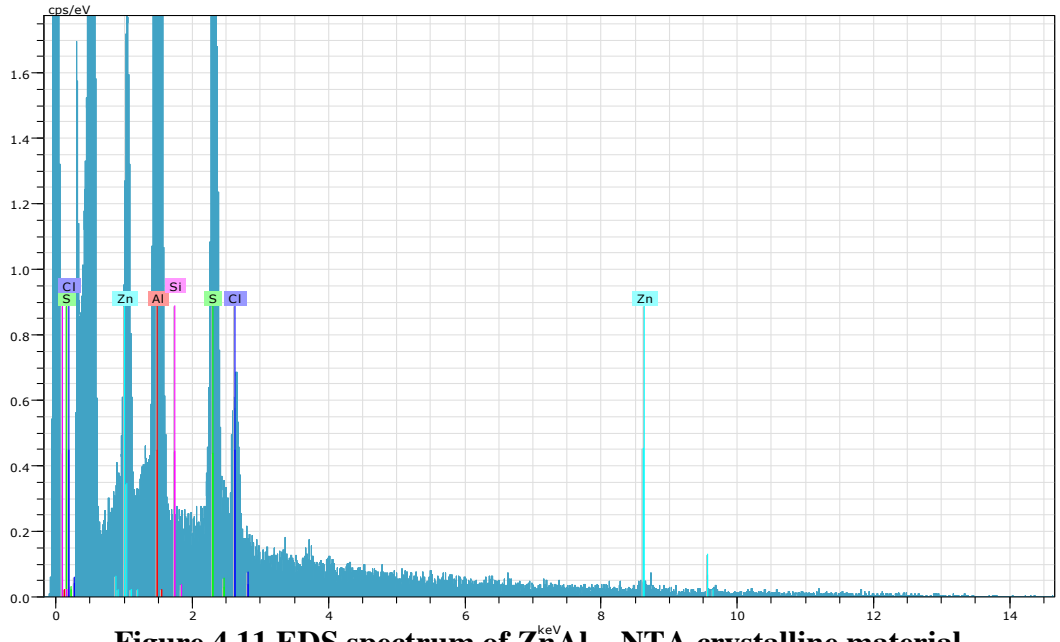

Figure 4.11 EDS spectrum of $ZnAl_{32}$-NTA crystalline material

In addition to that SEM/EDS were done on the post-TGA crystals as well. Figure 4.12 shows the SEM image of $CuAl_{30}$ sample after the thermo gravimetric analysis. As was expected the final material (confirmed by PXRD) is mostly amorphous, consisting of Aluminum, oxygen, copper and sulfur. (Figure 4.13) Even though it was expected to see a complete decomposition of 2, 6 NDS producing CO_2, H_2O and SO_x, the TGA data suggests the presence of residual sulfur in the compound. The elemental analysis data agrees with this as it confirms the presence of S in the final product. (Figure 4.13) On the other hand the SEM image of post-TGA $ZnAl_{32}$ sample too is completely amorphous as shown in Figure 4.14. EDS analysis of this material suggest the presence of zinc, aluminum, oxygen and sulfur elements. (Figure 4.15)

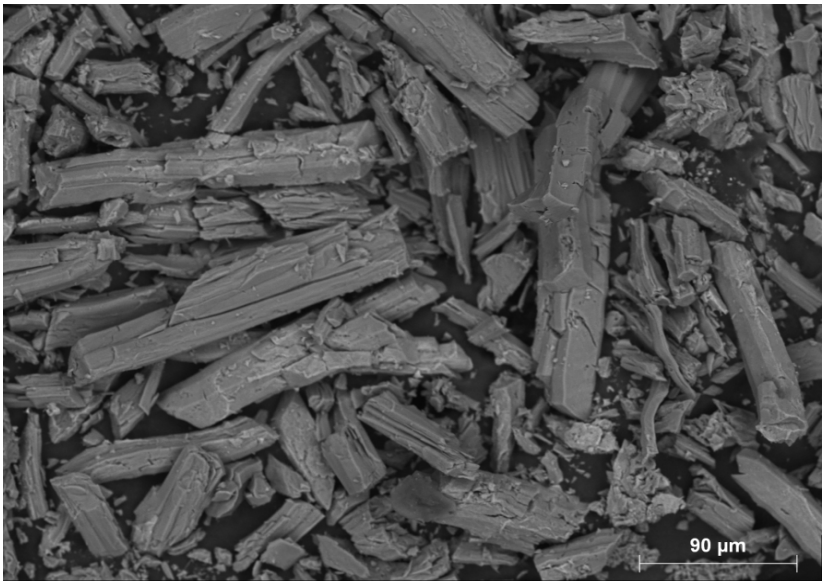

Figure 4.12 SEM image of the amorphous $CuAl_{30}$ after TGA

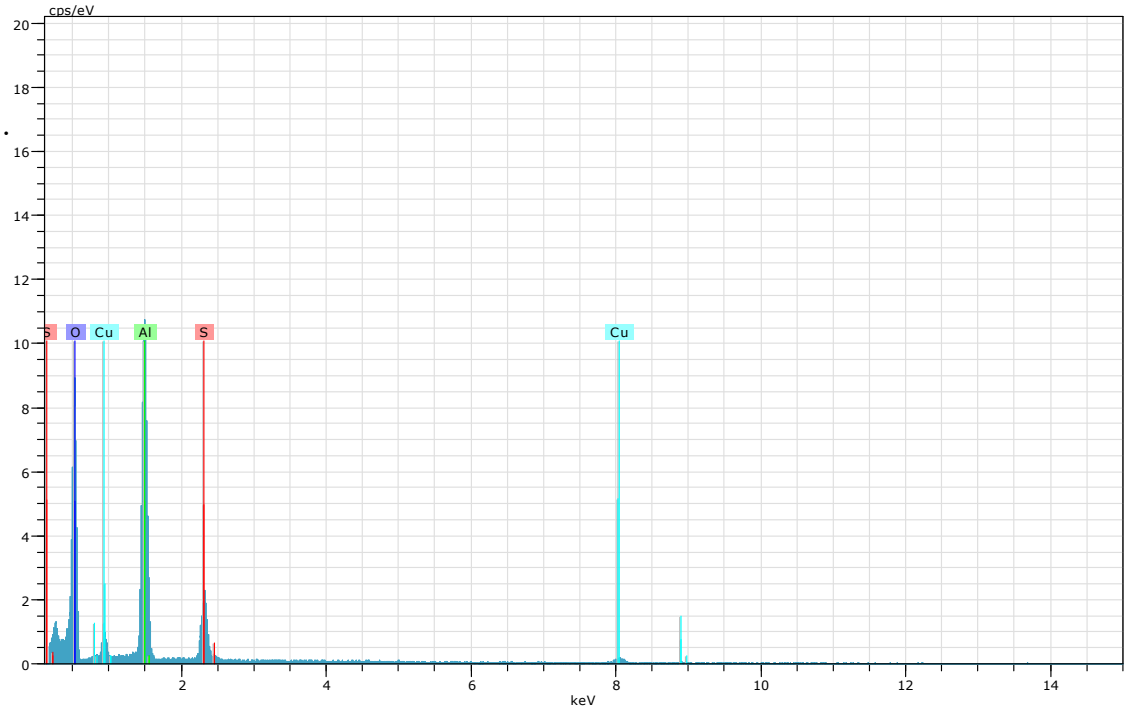

Figure 4.13 EDS spectrum of the amorphous $CuAl_{30}$ after TGA

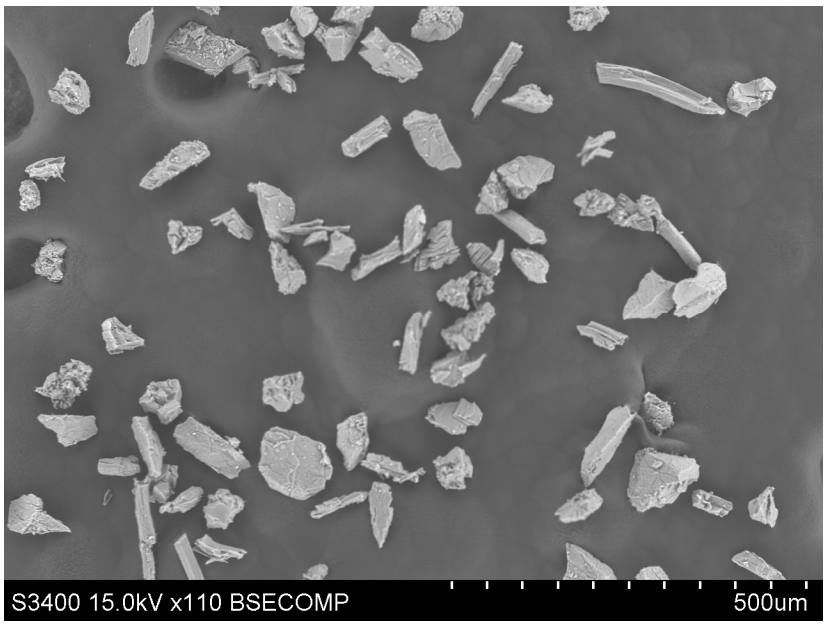

Figure 4.14 SEM image of amorphous post-TGA $ZnAl_{32}$-NTA

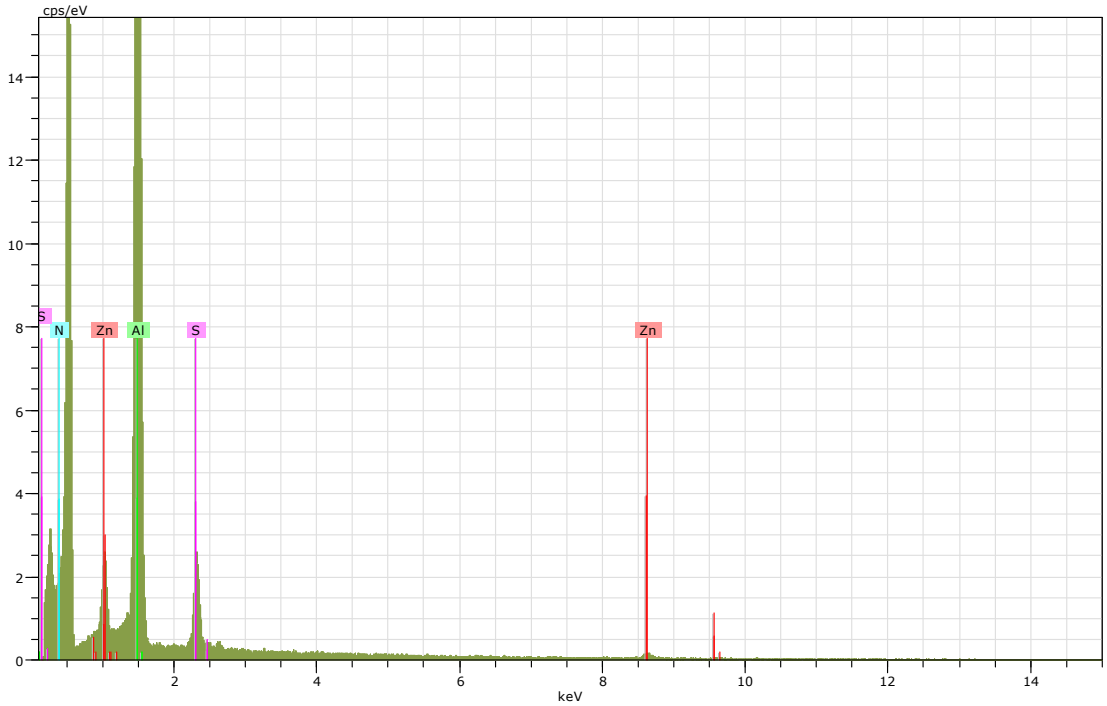

Figure 4.15 EDS spectrum of amorphous post-TGA $ZnAl_{32}$-NTA

4.6 Discussion

4.6.1 Adsorption of metal cations on to the Keggin-type aluminum clusters

This study reports the first ever synthesized polyaluminum cluster with heavy metal cations bonded to the exterior of the cluster. Pure-phase Al_{30} species can be crystallized from solution in the presence of a proper co-precipitating agent such as sulfate, selenate or 2,6 NDS[23]. $CuAl_{30}$ does not have any organic ligand bonded to the metal center whereas the $ZnAl_{32}$-NTA is bonded to the Zn^{2+} cation. In both of these species, the cations and the organics are bound to the octahedral aluminum atoms in the central belt in the polyaluminum cluster. Adsorption of IDA and sulfate (Sun et al.)[24] further suggest that this region of the cluster acts as the most reactive area where most of the species tend to adsorb.

The Keggin-type clusters have been suggested to occur in a variety of different environmental systems, but the most definitive evidence is found in the amorphous flocculants that precipitates from streams impacted by acid mine drainage. As the acidic waters from impacted streams flows into pristine waters, the rise in pH results in the formation of aluminum hydroxide colloids that aggregate into amorphous flocculants. During aggregation the flocculants trap other contaminants, such as Cu^{2+}, Zn^{2+}, Hg^{2+}, and Pb^{2+}, effectively controlling the fate and transport of these contaminants. In a 2005 study, Furrer et al, identified the epsilon-Al_{13} polynuclear species as a possible building block by 27-Al NMR spectroscopy. In addition, high-energy X-ray scattering data on amorphous aluminum hydroxide powders suggests that the delta-Al_{13} or the Al_{30} polynuclear species is more likely to be the structural component in this system (Forbes,

unpublished data). Thus our structural models have direct implications for increasing our molecular understanding of contaminant adsorption in natural systems.

Polyaluminum chloride coagulants, including $PACl_{Al30}$ that contains the Al_{30} cluster, are used to remove heavy metal contamination from wastewater stream. Our results again indicate that similar to the Al_{32}-IDA molecule, the Zn^{2+} and Cu^{2+} cations bond to the center of the Al_{30} cluster, suggesting a preferred adsorption site for contaminants on these molecules. An enhanced understanding of how these contaminants bind to coagulants could aid in developing novel materials and techniques for water purification.

CHAPTER 5

CONCLUSIONS AND FUTURE WORK

5.1 Conclusions

The **Al_{32}-IDA** compound is the first ever reported Keggin-type aluminum polycation that has been functionalized with an organic ligand. In addition **$CuAl_{30}$** and **$ZnAl_{32}$-NTA** are the first evidence for the coordination of heavy metal cations to a similar polyaluminum species. All these three compounds are important in gaining a molecular level understanding on how the removal of small organics and heavy metals occur via aluminum based coagulants in water purification processes. The ligands IDA, and the transition metal cations are all coordinated to the exterior of the cluster around the central area of the Al_{30} clusters, suggesting that this is the most active area with regard to adsorbing species into large polyaluminum species. The contribution of the co-precipitating agent 2,6-NDS is enormous in initializing the crystallization of these compounds.

Structural characterization is vital for deciphering the actual mechanism of the removal of contaminants from waste waters. In addition, it broadens our understanding of the hydrolysis of metal cations in aqueous media. The principle structural characterization method for these materials is the single crystal X-ray diffraction. And additional chemical characterization methods such as TGA, FTIR and SEM/EDS allowed us the estimation of the number of water molecules, verifying the presence of organics and elemental mapping respectively. Jahn Teller distortion around Cu^{2+} atom in $CuAl_{30}$ is also evident and it was supported by bond valence calculations and literature precedent.

A complete understanding of the role of coagulants in water purification is essential for the development of optimized coagulants which can enhance water purification.

5.2 Future Work

In this section I intend to describe the possible avenues that can be explored in this area of research. The findings in this research would undoubtedly enhance the understanding of the role of coagulants in waste water treatment. There are a couple of other things that we can do in order to gain further insight into this. To thorough our knowledge on the active site of these large aluminum species computational studies can be incorporated with the experimental findings. In fact, DFT calculations are currently being pursued as part of a collaborative project with Dr. Sarah Mason's group. Also for further verification of the environment around copper in $CuAl_{30}$ Electron Paramagnetic Resonance Spectroscopy (EPR) can be incorporated.

Similar experiments were carried out using other cationic species such as Ni^{2+} and Co^{2+} with identical conditions. However their behavior was different from the ones that are reported here. Evaluating thermodynamic and kinetic information for the synthesized compounds might be helpful in deciphering the factors accounting for this and to comprehend reactivity trends of these materials. Nano size inorganic species in aqueous systems play an important role in the transportation of heavy metal cations from the point source of contamination. Therefore these syntheses can be modified and extended to other heavy metal cations and also towards actinide materials such as thorium and uranium in order to gain a better understanding of the transportation of nuclear materials in the environment. This can probably be done by controlling the pH of the medium

which facilitates the formation of hydroxyl bridges conducive to the coordination of other chemical species.

Metal cation doped alumina and boehmite materials are well known for their catalytic activities. Therefore, these compounds can be further studied for their abilities to serve as molecular catalysts. Identification of more efficient co-precipitating agents will also be helpful in isolating novel crystalline materials. This might require different reaction conditions than those employed in our current studies. Some initial studies have been performed using a variety of mono and di sulfonate compounds although this requires further research.

REFERENCES

1. Cardarelli, F., *Materials handbook a concise reference of desktop*, 2nd Edition, Springer-Verlag London Limited, 2008.

2. Driscoll, C.T., Schecher, W.D., *Environmental Geochemistry and Health,* **1990**, 12, 28-49.

3. Stewart, T.A., D. Trudell, E., T.M. Alam, C.A. Ohlin, C. Lawler, W.H. Casey, S. Jett, and M. Nyman, *Environmental Science & Technology*, **2009**, 43, 5416-5422.

4. Hunter, D., Ross,D.S., *Science*, **1991**, 251,1056-1058.

5. Jolivet, J.P., Chaneac, C., Chiche, D., Cassaignon, S., Durupthy, O., Hernandez, J., *Comptes Rendus Geosciences*, **2011**, 343**,** 113-122.

6. Brosset, C., Biedermann, G., Sillen, L.G., *Acta Chemica Scandinavica*, **1954**, 8(10), 1917-1926.

7. Akitt, J.W., Lester, G.D., Khandelwal, B.L., Greenwood, N.N., *Journal of the Chemical Society-Dalton Transactions*, **1972**, 5, 604-610.

8. Akitt, J.W., Farthing, A., *Journal of the Chemical Society-Dalton Transactions*, **1981**, 7, 1624-1628.

9. Bottero, J.Y., Alexos, M., Tchoubar, D., Cases, J.M., Fripiat, J.J., Fiessinger, F., *Journal of Colloid and Interface Science*, **1987**, 117(1), 47-57.

10. Baes, C.F., Mesmer, R.E., The Hydrolysis of Cations, John Wiley and Sons, New York, 1976.

11. Smith, R.W., *Coordination Chemistry Reviews*, **1996**, 149, 81-93.

12. Kochian, L.V., *Annu. Rev. Plant Physiol. Plant Mol. Bio.*, **1995**, 46, 237-260.

13. Casey, W.H., B.L. Phillips, and G. Furrer, *Reviews in Mineralogy and Geochemistry*, **2001**, 44(1), 167-190.

14. Ohman, L-o., Forsling, W., *Acta Chem. Scand.,* **1981**, 35, 795-802.

15. Casey, W., H., *Chemical Reviews*, **2006**, 106(1), 1-16.

16. Feng, T.L., Gurian, P.L., Healy, M.D., Barron, A.R., *Inorganic Chemistry*, **1990**, 29, 408-411.

17. Sun, Z.,Wang, H., Feng, H., Zhang,Y., Du,S., *Inorganic Chemistry*, **2011**, 50(11), 9238-9242.

18. Furrer, G., Phillips, B. L., Ulrich, K. u., Pothig, R., Casey, W. H., *Science*, **2002,** 297, 2245-2247.

19. Desroches, S., Dayde, S., Berthon,G., *Journal of Inorganic Biochemistry*, **2000**, 81, 301-312.

20. Rowsell, J., Nazar, L.F., *Journal of the American Chemical Society*, **2000**, 122, 3777-3778.

21. Fu, G., Nazar, L.F., Bain, A.D., *Chem. Mater.* **1991**, 3, 602-610.

22. Allouche, L., Gerardin, C., Loiseau, T., Ferey, G., Taulelle, F., *Angewandte Chemie International Edition*, **2000**, 39(3), 511-514.

23. Abeysinghe, S., Unruh, D., Forbes, T.Z., *Crystal Growth and Design*, **DOI:** 10.1021/cg3000087.

24. Sun, Z., Wang, H., Tong, H., Sun, S., *Inorg. Chem.* **2011**, 50, 559-564.

25. J.P. Pineiro, A.M. Mota, M.F. Benedtti, *Environ. Sci. Technol.*, **2000**, 34, 5137.

26. Furrer, G., Phillips, B. L., Ulrich, K. u., Pothig, R., Casey, W. H., *Science*, **2002,** 297, 2245-2247.

27. Casey, W.H., M.M. Olmstead, B.L. Phillips, and L. Phillips, *Inorganic Chemistry*, **2005**, 44, 4888-4890.

28. Schmitt, W., E. Baissa, A. Mandel, C.E. Anson, and A.K. Powell, *Angewandte Chemie-International Edition*, **2001**, 40(19), 3577-3581.

29. Seichter, W., H.-J. Mogel, P. Brand, and D. Salah, *European Journal of Inorganic Chemistry*, **1998**, 795-797.

30. Armstrong, C.R., W.H. Casey, and A. Navrotsky, *Proceedings of the National Academy of Sciences of the United States of America*, **2011**, 108(36), 14775-14779.

31. Mainicheva, E.A., O.A. Gerasko, L.A. Sheludyakova, D.Y. Naumov, M.I. Naumova, and V.P. Fedin, *Russian Chemical Bulletin, International Edition*, 2006. **55**(2), 267-275.

32. West, A.R., Basic solid state chemistry, 2nd Edition, John Wiley and Sons. Ltd., West Sussex, England, 1999.

33. Massa, W., Crystal Structure determination, 2nd Edition, Springer, New York, 2004.

34. Hoft, R.W.W., *COLLECT*. 1998, Nonius B. V.: Delft, The Netherlands.

35. Bruker, APEXII, 1.2-27, Bruker AXS, madison, Wisconsin, USA. 2004.

36. Bruker, SADABS (version 2.0) and SHELXTL (version 6.1), Bruker AXS Inc., Madison, Wisconsin, USA,1998.

37. Tables, I.U.o.C.C.o.I., ed. *International Tables of Crystallography*, Wiley Publications: Oxford, England, 2006.

38. Spek, A.L., *Journal of Applied Crystallography*, **2003**, 36, 7-13.

39. Clegg, W. ed., Blake, A.J., Gould, R.O., Main, P., Crystal Structure analysis:Principle and practice, Oxford Science Publications, 2001.

40. Skoog, D.A, Holler, F.J., Nieman, T.A., Principles of Instrumental Ananlysis, 5th Edition, Thompson Learning, Inc., 1998.

41. Ngo, P.D., Wagner, L.C., (ed.), Failure Analysis of Integrated Circuits: Tools and Techniques, Kluwer academic Publishers, Norwell, Massachusetts, USA, 1999.

42. Brown, I.D., The chemical Bond in Inorganic Chemistry:The Bond Valence Model, Oxford University Press Inc., New York, 2002.

43. Brown, I.D., Journal of Chemical Education, 2000, 77(8), 1070-1075.

44. Yan, M.,Wang, D., Ni, J.,Qu, J., Chow, C.W.K., Hiu, H., *Water Research*, **2008**, 42, 3361-3370.

45. Hundt, T.R. and C.R. O'Melia, *Journal of the American Water Works Association*, **1988**, 80(4), 176-186.

46. Duan, J. and J. Gregory, *Advances in colloid and interface science*, 2003. **100-102**475-502.

47. Lothenbach, B., Furrer, G., Schulin, R., *Environ. Sci. Technol*., **1997**, 31, 1452-1462.

48. Wu, X., X. Ge, D. Wang, and H. Tong, *Colloids and Surfaces A*, **2007**, 30, 589-596.

49. Szabo-Bardos, E., Zsilak, Z., Lenvay, G., Horvath, O., Markovics, O., Hoffer, A., Toro, N, *Journal of Physical Chemistry B*, **2008**, 112, 14500-14508.

50. Jordan, P.A., N.J. Clayden, S.L. Heath, G.R. Moore, A.K. Powell, and A. Tapparo, *Coordination Chemistry Reviews*, **1996**, 149, 281-309.

51. Valle, G.C., Bombi, G.G., Corain, B., Favarato, M., Zatta, P., *Journal of the Chemical Society-Dalton Transactions*, **1989**, 1513-1517.

52. Powell, A K., Heath, S. L.,*Coordination Chemistry Reviews,* **1996,** 149, 59-80.

53. Petrosyants, S. P., Malyarik, M. A., Ilyukhin, A. B., *Zhurnal Neorganicheskoi Khimii* **1995,** 40, 769-775.

54. Hoveyda, H. R., Rettig, S. J., Orvig, C., *Inorganic Chemistry* **1993,** 32, 4909-4913.

55. Malone, S. A., Cooper, P., Heath, S. L., *Dalton Transactions,* **2003,** 4572-4573.

56. Schmitt, W., Jordan, P. A., Henderson, R. K., Moore, G. R., Anson, C. E., Powell. A. K., *Coordination Chemistry Reviews,* **2002,** 228, 115-126.

57. Duan, J., Gregory, J., *Advances in colloid and interface science*, **2003**, 100-102, 475-502.

58. Wang, W., Wentz, K.M., Hayes, S.E., Johnson, D.W., Keszler, D.A., *Inorganic Chemistry*, **2011**, 50(11), 4683-4685.

59. Vieno, N., Tuhkanen, T., Kronberg, L., *Environmental Technology*, **2006**, 27(2), 183-192.

60. Rustad, J., *Geochimica Et Cosmochimica Acta*, **2005**, 69(18), 4397-4410.

61. Harsh, J.B., Doner, H.E., *Soil.Sci.Soc.Am.J.,* **1984**, 48, 1034-1039.

62. Furrer, G., *Aquat. Sci.*, **1993**, 55, 281-290.

63. Coronado, E., Gomez-Garcia, C.J., *Chemical Reviews*, **1998**, 98(1), 273-296.

64. Putaj, P., Lefebvre, F., *Coordination Chemistry Reviews*. **255**(15-16), 1642-1685.

65. Johansson, G., *Acta Chemica Scandinavica,* **1960**, 14, 771-773.

66. Rademeyer, M., *Acta Cryst.*, **2004**, E60, m993- m995.

67. Liu, H., Song, L-j., Ju, Z-f., Li, W., Zhang, J., *Journal of Molecular Structure,* **2008**, 875, 565–569.

68. Yasodha, V., Govindarajan, S., Low, J.N., Glidewell, C., *Acta Cryst.,* **2007**, C63, m207- m215.

69. Li, L., Liu, B., Xue, G., Hu, H., Fu, F., Wang, J., *Crystal Growth and Design*, **2009**, 9, 5206-5212.

70. Keene, T.D., Hursthouse, M.B., Price, D.J., *Z. Anorg. Allg. Chem.* **2004**, *630*, 350-352.

71. Kawata, S., Kumagai, G., Adachi, K., Kitagawa, S., *J. Chem. Soc., Dalton Trans.*, **2000**, 2409–2417.

72. Choudhury, S.R., Bhattacharyya, J., Das, S., Dey, B., Mukhopadhyay, S., Lu, L-p., Zhu, M-l., *Acta Cryst.*, **2007**, E63, m1331–m1332.

73. Zhang, X-y., *Acta Cryst.*, **2007**, E63, m1254–m1255.

74. Yan, B., Goh, N.K., Chia, L.S., *Inorganica Chimica Acta*, **2004**, 357, 490–494.

75. Guo, Q-l., Zhu, W-x., Ma, S-l., Dong, S-j., Xu, M-q., *Polyhedron*, **2004**, 23, 1461–1466.

76. Rodriguez-Martin, Y., Sanchiz, J., Ruiz-Perez, C., Lloret, F., Julve, M., *Cryst. Eng. Comm.,* **2002**, 4(107), 631–637.

APPENDIX

Table A1: Bond Valence Table - $CuAl_{30}$

B = 0.37 Al R_0 = 1.620; Allman (1975)

	Al1	Al2	Al3	Al4	Al5	Al6	Al7	Al8	Al9	Al10	Al11	Al12	Al13	Al14	Al15	Cu1	S2	B.V.	dentity
O1						0.528					0.562							1.09	OH
O2	0.562					0.497												1.06	OH
O3					0.507	0.487												0.99	OH
O4														0.541	0.564			1.11	OH
O5		0.597														0.412		0.60	H2O
O6						0.423												0.42	H2O
O7				0.546				0.503										1.05	OH
O8	0.526		0.506															1.03	OH
O9		0.512	0.487															1.00	OH
O10					0.517				0.520									1.04	OH
O11		0.521	0.490															1.01	OH
O12	0.567							0.493										1.06	OH
O13							0.434											0.43	H2O
O14													0.490		0.498			0.99	OH
O15							0.411					0.645		0.294	0.372			1.72	O
O16							0.519				0.570							1.09	OH
O17								0.494					0.534					1.03	OH
O18									0.536				0.534					1.07	OH
O19				0.561			0.470											1.03	OH
O20										0.555				0.568				1.12	OH
O21			0.482								0.520							1.00	OH
O22								0.482	0.509									0.99	OH
O23	0.395			0.354							0.356	0.556						1.66	O
O24			0.414															0.41	H2O
O25													0.546		0.530			1.08	OH
O26				0.550												0.443		0.55	H2O
O27	0.402	0.443		0.410														1.26	OH
O28		0.400		0.420							0.411							1.23	OH
O29														0.427				0.43	H2O
O30								0.411	0.320			0.623	0.344					1.70	O
O31						0.499				0.524								1.02	OH
O32										0.523				0.527				1.05	OH
O33							0.485							0.534				1.02	OH
O34							0.502								0.499			1.00	OH
O35			0.383															0.38	H2O
O36					0.541					0.572								1.11	OH
O37					0.524				0.521									1.05	OH
O38								0.436										0.44	H2O
O40																0.073	1.644	1.72	O
O45	0.404	0.410									0.405							1.22	OH
O46													0.417					0.42	H2O
O47					0.422													0.42	H2O
O48															0.422			0.42	H2O
O49																0.389		0.39	H2O
O50																0.351		0.35	H2O
O60					0.351	0.411				0.303		0.658						1.72	O
O67									0.434									0.43	H2O
O68										0.414								0.41	H2O
O81																0.076		0.08	H2O
B.V.	2.8560	2.8829	2.7627	2.8410	2.8638	2.8460	2.8204	2.8190	2.8392	2.8904	2.8248	2.4826	2.8646	2.8919	2.8850	1.6690			
IDEAL	3	3	3	3	3	3	3	3	3	3	3	3	3	3	3	2			

Table A2: Bond Valence Table - $ZnAl_{32}$-NTA

Bond Valence Table

B = 0.37 Al R_o = 1.620; Allman (1975)

	Al1	Al2	Al3	Al4	Al5	Al6	Al7	Al8	Al9	Al10	Al11	Al12	Al13	Al14	Al15	Al16	Zn1	B.V.	Identity
O1											0.296		0.330	0.421		0.637		1.68	O
O2			0.501	0.568														1.07	OH
O3		0.567	0.487															1.05	OH
O4						0.552												0.55	H2O
O5				0.553										0.483				1.04	OH
O6											0.531	0.550	0.550					1.63	O
O7		0.533					0.469											1.00	OH
O8						0.517	0.467											0.98	OH
O9										0.530		0.537						1.07	OH
O10	0.516							0.537										1.05	OH
O11			0.387							0.340		0.320				0.625		1.67	O
O12		0.393		0.334		0.344										0.561		1.63	O
O13									0.539		0.523							1.06	OH
O14					0.436			0.524										0.96	OH
O15							0.421		0.301					0.315		0.607		1.64	O
O16									0.528						0.543			1.07	OH
O17	0.493																	0.49	H2O
O18							0.473		0.512									0.98	OH
O19							0.436											0.44	H2O
O20										0.513	0.422							0.94	OH
O21									0.431									0.43	H2O
O22			0.472															0.47	H2O
O23			0.514									0.507						1.02	OH
O24	0.453																	0.45	H2O
O25							0.477								0.498			0.97	OH
O26														0.440				0.44	H2O
O27									0.528		0.527							1.06	OH
O28					0.458			0.526										0.98	OH
O29		0.370		0.417				0.446										1.23	OH
O30			0.448															0.45	H2O
O31																	0.362	0.36	H2O
O32					0.469												0.497	0.97	OH
O33												0.531			0.531			1.06	OH
O34												0.502			0.524			1.03	OH
O35		0.394				0.404		0.383										1.18	OH
O36													0.418					0.42	H2O
O37				0.498	0.479													0.98	OH
O38				0.411		0.386		0.400										1.20	OH
O39		0.544			0.472													1.02	OH
O40										0.495			0.526					1.02	OH
O41	0.463					0.460												0.92	OH
O42	0.460																	0.46	H2O
O43					0.393													0.39	H2O
O44											0.543			0.516				1.06	OH
O46													0.485	0.468				0.95	OH
O48										0.394								0.39	H2O
O50										0.533			0.510					1.04	OH
O53												0.428						0.43	H2O
O55																	0.315	0.31	H2O
O56																	0.343	0.34	H2O
O65															0.427			0.43	H2O
O68																	0.308	0.31	H2O
B.V.	2.3846	2.8000	2.8094	2.7810	2.7070	2.6638	2.7430	2.8157	2.8396	2.8045	2.8426	3.3757	2.8186	2.6432	2.0963	2.4289	1.8237		
IDEAL	3	3	3	3	3	3	3	3	3	3	3	3	3	3	3	3	2		